Porosity and Permeability Prediction through Forward Stratigraphic Simulations Using GPM™ and Petrel™: Application in Shallow Marine Depositional Settings.

Daniel Otoo and David Hodgetts

Department of Earth and Environmental Sciences, University of Manchester, Manchester, M13 9PL, United Kingdom.

Correspondence to: Daniel Otoo (daniel.otoo@manchester.ac.uk)

Abstract

The forward stratigraphic simulation approach ~~was used~~is applied to ~~model~~forecast porosity and permeability ~~attributes~~trends in the Volve field~~, Norway. This was achieved by applying spatial data~~ subsurface model. Variograms and synthetic well logs from the forward stratigraphic ~~simulation to control property distribution in the reservoir~~ model~~.~~ were combined with known data to guide porosity and permeability distribution. Building a reservoir model that fits data at different locations ~~is a task associated~~comes with high levels of uncertainty. ~~To minimise property representation uncertainties in a reservoir model, geologically realistic sediment distribution patterns must be developed~~Therefore, it is critical to ~~predict~~generate an appropriate stratigraphic framework to guide lithofacies ~~units~~ and associated petrophysical ~~properties.~~distribution in a subsurface model. The workflow adopted is in three parts; first, ~~the~~ simulation of twenty scenarios of sediment transportation and deposition using the geological process modeling (GPM™) software developed by Schlumberger ~~was used to simulate scenarios of sediment transportation and deposition in the model area.~~. Secondly, an estimation of the extent and proportion of lithofacies proportions in the stratigraphic model ~~was done~~ using the property calculator tool in ~~the~~ Petrel™ ~~software~~. Finally, porosity and permeability values were assigned to corresponding lithofacies-associations in the forward stratigraphic model to produce a forward stratigraphic-based ~~petrophysical model.~~porosity and permeability models. Results show a lithofacies distribution ~~that is controlled by~~model, which depends on sediment diffusion rate, sea level variation, flow rate, wave processes, and tectonic events. This observation is consistent with ~~real-world events, were~~the natural occurrence, where variation

in sea level, ~~volume of~~ sediment ~~input~~supply, and accommodation control ~~the build-up of~~ stratigraphic ~~sequence~~sequences. Validation wells, VP1 and VP2 located in the original Volve field ~~petrophysical~~ model and the forward stratigraphic-based models show a ~~good match in porosity and permeability attributes at 5 m vertical sample intervals. The resultant forward stratigraphic-based porosity and permeability models suggests~~significant similarity, especially in the porosity models. These results suggest that forward stratigraphic simulation outputs can be ~~integrated into classical~~used together with geostatistical modeling workflows to improve subsurface property representation~~, and well planning strategies.~~ in reservoir models.

Introduction

The distribution of reservoir properties such as porosity and permeability is a direct function of a complex combination of sedimentary, geochemical, and mechanical processes (Skalinski & Kenter, 2014). The impact of reservoir petrophysics on well planning and ~~extraction~~production strategies makes it imperative to use reservoir modeling techniques that present realistic property variations ~~in~~via 3-D models (Deutsch and Journel, 1999; Caers and Zhang, 2004; Hu & Chugunova, 2008). Typically, reservoir modeling ~~require~~ requires continued property modification until an ~~a~~ appropriate match to ~~known~~ subsurface data ~~is obtained.~~ ~~However, acquisition of~~. Meanwhile, subsurface ~~datasets~~ data acquisition is ~~costly,~~ expensive, thus restricts data collection and accurate subsurface property modeling ~~conditions.~~. Several studies, ~~e.g.~~ Hodgetts et al. (2004) and Orellana et al. (2014) have demonstrated ~~that~~how stratigraphic patterns, and therefore petrophysical attributes ~~can be extrapolated from~~ in seismic~~, outcrop~~ data, outcrops, and well logs~~.~~ are applicable in subsurface modeling. However, ~~this notion is limited by~~ the absence of ~~accurate and reliable~~ detailed 3-~~D~~dimensional depositional ~~models~~frameworks to guide property modeling ~~in reservoir units~~ inhibits this strategy (Burges et al. 2008). Reservoir modeling techniques with the capacity to integrate forward stratigraphic simulation outputs with stochastic modeling techniques for subsurface property modeling will improve reservoir heterogeneity characterization, because they more accurately produce geological realism than the other modeling methods (Singh et al. 2013). The use of geostatistical-based methods to represent ~~the~~ spatial variability of reservoir properties ~~have~~has been ~~widely accepted~~ in many exploration and production projects (~~e.g.~~ Kelkar and Godofredo, 2002). In the geostatistical modeling ~~methods~~method, an alternate numerical 3-D model (~~i.e.~~ realizations) ~~is derived to demonstrate~~shows different ~~scenarios of~~ property distribution scenarios that ~~can be conditioned~~

are most likely to match well data (Ringrose & Bentley, 2015). ~~Reservoir modeling practioners are normally faced with~~However, due to cost reservoir modeling practitioners continue to encounter the challenge of ~~getting a lot of~~ obtaining adequate subsurface data to deduce reliable ~~variogram models as a result of cost,~~ variograms for subsurface modeling, therefore introducing a significant level of uncertainty in ~~a~~ reservoir ~~model~~models (Orellena et al. 2014). The advantages of applying geostatistical modeling approaches ~~in populating propoerties~~to represent reservoir properties in models are discussed in ~~reservoir models is well established (e.g.~~ studies by Deutsch and Journel~~,~~ (1999~~;~~), Dubrule, (1998~~), but~~). A notable disadvantage is that the geostatistical~~-based~~ modeling method tends to confine -reservoir -property ~~-models~~ distribution to ~~-known~~ subsurface data -and -rarely ~~-realize~~ produces geological -realism -to capture sedimentary events that ~~have~~ led to reservoir formation (Hassanpour et al. 2013). In effect, the geostatistical

4

modeling technique ~~is unable to~~does not reproduce ~~a~~ long-range continuous reservoir properties ~~that~~, which are essential for generating realistic reservoir connectivity models (Strebelle & Levy, 2008). ~~Based~~ The forward stratigraphic simulation approach was applied in this contribution to forecast lithofacies, porosity, and permeability in a reservoir model, based on lessons from ~~a previous work (e.g.~~ Otoo and Hodgetts~~,~~ (2019~~), the forward stratigraphic simulation approach was applied in this contribution to predict lithofacies units, porosity, and permeability properties in a 3-D model. An important~~). A significant aspect of this work is ~~the use of~~using variogram parameters from forward stratigraphic-based synthetic wells to ~~populate petrophysical properties~~simulate porosity and permeability trends in the reservoir model ~~grid~~. Forward stratigraphic modeling involves ~~the uses~~ morphodynamic rules to ~~derive sedimentary~~ replicate 3-dimensional stratigraphic depositional trends ~~to reflect~~ observed in data (e.g. seismic). Forward stratigraphic ~~patterns in known data. The approach is driven by~~modeling operates on the guiding principle that multiple sedimentary process-based simulations in a 3-D framework will improve facies, and therefore petrophysical property distribution in a geological model.

The geological process modeling GPM^{TM} software (Schlumberger, 2017), which operates on forward stratigraphic simulation principles, replicates a depositional sequence to provide a 3-dimensional framework to predict porosity, permeability in the study area. The reservoir interval under study is ~~located~~ within the Hugin formation. Studies by Varadi et al. (1998); Kieft et al. (2011~~), suggest~~) indicate that the Hugin formation ~~consist~~consists of a complex depositional architecture of waves, tidal, and fluvial processes. This ~~indicates~~knowledge suggests that a single depositional model will not be adequate to produce a ~~realisite~~realistic lithofacies or petrophysical distributions model of the area. Furthermore, the complicated Syn-depositional rift-related faulting system, significantly ~~influence~~influences the stratigraphic architecture (Milner and Olsen, 1998). ~~The~~ Therefore, the focus ~~of this work~~here is to produce a depositional sequence ~~in the shallow marine environment by using~~

~~a forward stratigraphic modeling approach~~, which captures subsurface attributes observed in ~~the GPM™ (Schlumberger, 2017),~~ seismic and ~~use variogram~~well data to guide property modeling.

~~parameters from the forward model to control porosity and permeability property representation in the Volve field model grid.~~

Study Area

The Volve field (Figure 1), located in Block 15/9 south of the Norwegian North Sea ~~is Jurassic in age (i.e. late Bajocian to Oxfordian) with~~, has the Hugin Formation as the ~~main~~ reservoir ~~unit~~interval from which hydrocarbons are produced (Vollset and Dore, 1984). The Hugin formation, which is Jurassic in age (late Bajocian to Oxfordian), is made up of shallow marine to marginal marine sandstone deposits, coals, and a significant influence of wave events that tend to control lithofacies distribution in the formation (Varadi et al. 1998; and Kieft et al. 2011). ~~Several studies, e.g.~~Studies by Sneider et al. (1995~~),~~) and Husmo et al. (2003) associate sediment deposition ~~in~~into the ~~Hugin system~~ study area to

~~a~~ rift-related subsidence and successive flooding during a large transgression of the Viking Graben within the Middle to Late Jurassic period. Also, Cockings et al. (1992), Milner and Olsen (1998) indicate that the Hugin formation comprises of marine shoreface, lagoonal and associated coastal plain, back-stepping delta-plain, and delta front. However, recent studies by Folkestad and Satur (2006) also provide evidence of a high tidal event, which introduces another dimension that requires attention in any subsurface modeling task in the study area. The thickness of the Hugin formation is estimated between 5 m and 200 m, but can be thicker off-structure and non-existent on structurally high segments due to post-depositional erosion (Folkestad and Satur, 2006).

~~the Middle to Late Jurassic period. Previously it was interpreted to comprise of marine shoreface, lagoonal and associated coastal plain, back-stepping delta-plain and delta front deposits (e.g. Cockings et al. 1992; Milner and Olsen, 1998), but recent studies, e.g. Folkestad and Satur, (2006) suggest the influence of a strong tidal event, which introduces another dimension in property modeling of the reservoir. The thickness of the Hugin formation is estimated to range between 5 m and 200 m but can be thicker off-structure and non-existent on structurally high segments as a result of post-depositional erosion (Folkestad and Satur, 2006).~~

~~Based on studies by Kieft et al. (2011), a~~A summarised sedimentological delineation within the Hugin formation is ~~presented in~~ derived based on studies by Kieft et al. (2011). In **Table 1**~~. Lithofacies,~~ lithofacies-association codes A, B, C, D, and E ~~used in the classification represents~~ represent bay fill units, shoreface sandstone facies, mouth bar units, fluvio-tidal channel fill sediments, and coastal plain facies units, respectively. ~~In addition~~ Additionally, a lithofacies association prefixed code F ~~was interpreted to consist~~, which consists of open marine shale units, mudstone ~~with~~. Within it are occasional siltstone beds, parallel laminated soft sediment deformation that locally develop at bed tops. The lateral extent of the code F lithofacies package in the Hugin formation is estimated to be 1.7 km to 37.6 km, but the total thickness of code F lithofacies is not known (Folkestad & Satur, 2006).

Data and Software

This work is based on the description~~,~~ and interpretation of petrophysical datasets in the Volve field by ~~Statoil, now~~ Equinor. Datasets include 3-D seismic ~~sections,~~ and a suite of 24 wells that consist of formation pressure data, core data, petrophysical and sedimentological logs. Previous ~~works such as~~studies by Folkestad & Satur~~,~~ (2006) and Kieft et al~~.~~., (2011) in this reservoir interval show varying grain size, sorting, sedimentary structures, bounding contacts of sediment matrix ~~that play a significant part of the reservoir petrophysics.~~. Grain size, sediment matrix, and the degree of sorting will typically drive the volume of the void created, and therefore the porosity and permeability attributes~~-~~. Wireline-log attributes such as gamma~~-~~-ray (GR), sonic (DT), density (RHOB), and neutron-porosity (NPHI) ~~were used to~~ distinguish lithofacies units, stratigraphic horizons, and zones that are ~~required to build~~essential for building the 3-D property model~~. Porosity, and permeability models, of the Volve field,~~

~~were generated~~ in Schlumberger's Petrel™ software. ~~Importantly,~~ Besides, this ~~work~~study also seeks to produce ~~geologically~~ a realistic depositional ~~architecture that is comparable to a real-world~~model like the natural stratigraphic framework in a shallow marine ~~environment. Deriving a representative~~ depositional setting. Therefore, obtaining a 3~~-D stratigraphic model of the reservoir~~dimensional stratigraphic model that shows a similar stratigraphic sequence observed in the seismic data allows us to deduce variogram parameters to serve as input in actual subsurface property modeling.

~~allows us to deduce geometrical and variogram parameters as input datasets in actual subsurface property modeling.~~

~~Schlumberger's~~ Twenty forward stratigraphic simulations were produced in the geological process modeling (GPM™) software ~~was used to undertake twenty forward stratigraphic simulation in an attempt to replicate~~to illustrate depositional processes that resulted in the build-up of the reservoir interval under study. ~~Simulations were constrained to twenty scenarios because the desired stratigraphic sequence and associated sediment patterns were achieved at~~By the fourth simulation~~. The main criteria for evaluating the realistic nature~~, there was a development of ~~a~~ stratigraphic ~~model was to compare it to~~patterns that shows similar sequences as those observed in seismic, hence the ~~depositional sequence observed in the seismic section in Figure 3b. Several process modeling software packages exist and have been applied in similar studies; e.g.~~decision to constrain the simulation to twenty scenarios. Delft3D-Flow™; Rijin & Walstra, (2003); DIONISOS™; Burges et al. (2008~~). The geological~~) are examples of subsurface process modeling ~~(GPM™)~~ software ~~was preferred because of the~~ used in similar studies. The availability of the GPM™ software license~~,~~ and ~~also~~ the ~~ease in integrating of its~~capacity to integrate stratigraphic simulation outputs ~~into~~in the property modeling workflow in Petrel™~~.~~ is the reason for using the geological process modeling software in this study.

Methodology

The workflow (Figure 2a) combines the stratigraphic simulation capacity of ~~the~~ GPM™ ~~software~~ in different ~~depositional settings,~~ sedimentary processes and the property modeling tools in Petrel™ to predict the distribution of porosity and permeability properties away from ~~well~~known data. ~~Three~~This involves three broad ~~steps have been used here to achieve this goal;~~: (i) forward stratigraphic simulation ~~(FSS)~~ in GPM™ ~~software~~ (2019.1 version), (ii) lithofacies classification using the calculator tool in Petrel™, and (iii) ~~lithofacies,~~ porosity~~,~~ and permeability modeling in Petrel™ (2019.1 version).

~~Process Modeling~~Forward Stratigraphic Simulation in GPM™

The GPM™ software ~~consist~~consists of different geological processes ~~that are designed~~ to replicate sediment deposition in clastic and carbonate environments. ~~For example, previous studies, e.g.~~ Kieft et al~~,~~. (2011)

in their work in this area, identified the influence of ~~riverine (~~fluvial~~),~~ and wave processes in the genetic structure of sediments in the Hugin formation. These geological processes ~~could be~~are very rapid, depending on accommodation generated ~~as a result of~~ by sea~~-~~-level variation~~,~~ and or sediment composition and flow intensity. ~~Sediment~~ The deposition~~,~~ of sediments into a geological basin and its response to post-depositional sedimentary ~~and~~or tectonic processes are significant in the ultimate distribution of subsurface lithofacies ~~units. To attain stratigraphic outputs that fall within the depositional architecture captured in the seismic section (Figure 3b), the~~ and petrophysics. Therefore, different input parameters ~~were varied as illustrated by different scenarios in Table 2. The~~ for the forward simulation ~~generated geologically realistic stratigraphic trends, but~~to attain a stratigraphic output that fits existing knowledge of paleo-sediment transportation and deposition into the study area (see Table 2). The forward simulation at all stages portrayed geological realism concerning stratigraphic sequence, but it also revealed some limitations, such as instability in the simulator when more than three geological processes ~~and sub-operations~~ run ~~at a time. In view of~~concurrently. Given this, the diffusion and tectonic processes ~~were combined with other processes such as~~ remained constant, whiles varying the steady flow, unsteady flow, and sediment accumulation ~~to~~processes at each run.

~~replicate the Volve field stratigraphic depositional scenarios.~~

Steady & Unsteady Flow Process

The steady flow process in GPM ~~simulate~~simulates flows that ~~changes~~change slowly over a period, or sediment transport scenarios where flow velocity and channel depth do not vary abruptly~~;~~ e.g.~~.~~., rivers at a normal stage, deltas, and sea currents. The steady flow process can be specified to ~~a~~the desired setting in the “run sedimentary simulation” dialog box in the Petrel™ software (version 2017.1 and above). Considering the influence of fluvial activities during sedimentation in the ~~build-up of the~~ Hugin formation, it ~~was important~~is significant to capture its impact on the resultant simulated output. ~~To attain stability in the simulator, it is advisable to undertake preliminary~~

~~runs to ascertain the appropriateness of input parameters that will be used in the simulation. For steady~~ ~~flow process, a~~ A boundary condition ~~must be~~is specified at the edges of the model~~.~~ structure to guide sediment and fluid movement in the model. For example~~ in~~ , where the boundary condition is an open flow system, negative integers (~~i.e.~~ values below zero) must be assigned to the edges of the hypothetical paleo-surface to allow water to enter and leave the ~~simulation~~ area~~.~~ of interest.

~~Unsteady Flow Process~~

The unsteady flow process can ~~model flows that are~~ simulate periodic~~,~~ flows and run for a limited time; for example, in turbidites where the velocity of flow and depth changes abruptly over time. The unsteady flow process algorithm ~~is set up to apply a number of~~ applies several fluid elements~~, that are affected~~ driven by gravity~~,~~ and ~~by~~ friction against the hypothetical topographic surface. ~~A contribution on the application of the unsteady in stratigraphic simulation, and how its settings can be configured to attain geological realistic outcomes is discussed in~~ In Otoo and Hodgetts~~,~~ (2019~~).~~), is an account of how the unsteady process in GPM™ attains realistic distribution of lithofacies units in a turbidite fan system. The steady and unsteady flow processes are based on simplified Navier-Stokes equations to represent flows in channels and pathways that have irregular cross-sections and or channels that converge as tributaries or diverge as distributaries such as turbidite flow. The simplified Navier-Stokes comprises of two key parameters that partly rely on channel geometry and flow velocity. The Navier-Stokes equation combines the continuity equation (2) and the momentum equation (3) to generate the equation on which the steady and unsteady flow processes evolve.

The continuity equation integrates the conservation of mass:

$$\frac{\partial \rho}{\partial t} + \nabla.\rho \mathrm{q} = 0 \qquad (1)$$

Where ρ is fluid density, t is time, and q the flow velocity vector.

The equation that shows the changes in momentum by the fluid:

$$\mathrm{p}.\left(\frac{\partial q}{\partial t} + (q.\nabla)q\right) = -\nabla\rho + \nabla.\mu U + \rho(g + \Omega q) \qquad (2)$$

Where P is pressure, t is time, μ is fluid viscosity, and U is the Navier Stokes tensor.

Keeping density (ρ) and viscosity (μ) as constant, a simple flow equation is obtained:

$$\frac{\partial q}{\partial t} + (\mathrm{q}\ .\nabla)\mathrm{q} = -\nabla\Phi + \mathrm{v}\nabla^2\mathrm{q} + \mathrm{g} \qquad (3)$$

Where, Φ is the ratio of pressure to constant density (i.e. P/ρ), and v is the kinematic viscosity (i.e. μ/ρ)

The solution of the framework formed in (3) is completely obtained by specifying various boundary conditions that are used in the steady and or unsteady flow processes.

A full description of equations that form the building block for sediment movement under steady and unsteady flow processes in the simulator is available in Tetzlaff & Harbaugh (1989).

Sediment Diffusion Process

The diffusion process can effectively replicate sediment ~~erosion~~movement from ~~areas of~~a higher slope (~~i.e.~~ source location) and ~~their~~its deposition ~~to~~into a lower elevation of the model area. Sediment ~~dispersion~~movement in the diffusion process is ~~carried out~~ through erosion and transportation processes that are driven by gravity ~~in the simulator. The~~. Sediment diffusion ~~process is based~~runs on the assumption that sediments are transported downslope at a proportional rate to the topographic gradient~~; therefore~~, making fine-grained sediments easily transportable than coarse-grained sediments. ~~Diffusion is controlled by two~~ Sediment diffusion depends on three parameters~~;~~: (i) ~~diffusion coefficient, which controls the strength of the diffusion, and~~sediment grain size and turbulence in the flow (ii) diffusion coefficient, and (iii) diffusion curve that serves as a unitless multiplier in the algorithm. ~~The governing equation for the~~Based on Dade & Friend (1998); and Zhong (2011), a mathematical summary of the influence these factors have on the resultant diffusion ~~process is~~profile is derived. Considering that the grain size for each sediment component (coarse sand, fine sand, silt, and clay) are known, the assumption is that these particles have a uniform diameter (D) in the flow mix. In that case, external fore (F_e), which consist of drag, lift, virtual mass, and Basset history force is given as:

$$\cancel{\frac{\partial z}{\partial t} = k\nabla^2 z,}\ F_e = \alpha_e M_e + \alpha_e \Phi_D.\frac{U_{fi}-U_{ei}}{T_p} \qquad (4)$$

M_e is the resultant force of other forces with the exception of drag force, T_p stokes relation time, expressed as: $T_p = \rho_\rho D^2/(18\rho_f V_f)$, with ρ_f and V_f as density and viscosity of fluid respectively. Φ_D is a coefficient that accounts for the non-linear dependence of drag force on grain slip Reynolds number (R_p).

$$\Phi_D = \frac{Rp}{24} C_D \qquad (5)$$ with C_D sediment grain coefficient.

With the flow component in place, the diffusion coeff icient (D_i) is deduced from the Ei nstein equation. Using an assumption that the diffusion coefficient decreases with increasing grain size and rise in temperature, and that the coefficient f is known, the expression for D_i is:

$$D_i = \frac{K_B.T}{f} \qquad (6)$$

Meanwhile, f is a function of the dimension of the spherical particle involved at a particular time (t). In accounting for f, the equation for D_i changes into:

$$D_i = \frac{K_B.T}{6.\pi.\eta_o.r} \qquad (7)$$

The rate diffusion of diffusion relative to topography in the simulator is achieved through;

$$\frac{\partial z}{\partial t} = D_i \nabla^2 z \qquad (8)$$

where **z** is topographic elevation, **k** the diffusion coefficient, **t** for time, and ~~$\nabla^2 z$~~ $\nabla^2 z$ is the laplacian.

Sediment Accumulation

In ~~the~~ GPM™ ~~software~~, sediment source can be set to a point location or considered to emanate from a whole area. Sediment accumulation ~~deals with~~ represents sediment deposition ~~via~~ through an areal source. For example, where a lithology is ~~interpreted to be uniformly distributed~~ distribution is invariable, the sediment accumulation process can ~~be used to~~ replicate such a depositional scenario. The areal input rates for each sediment type (~~e.g.~~ coarse grained, fine grained sediments) ~~used in the accumulation process must be specified in the settings. Specifying the areal rates for each sediment is important because the software is configured to~~ use the value of the surface at each cell in the model grid and ~~multiplies~~ multiply it by ~~–~~a value ~~(i.e. value~~ from a unitless curve~~)~~ at each time step in the simulation to estimate the thickness of sediments accumulated or eroded from a cell in the model. Based on Tetzlaff & Harbaugh (1989), the equation for estimating sediment accumulation is given:

~~Parameters~~ $$(H - Z)\frac{Dl_{Ks}}{Dt} = f(Q, \nabla H, \nabla Z, L, F, K_s, k(Z)) \qquad (9)$$

Where;

H is the free surface elevation to sea level, Z is the topographic elevation for sea level, K_s is the sediment type, $l_{ks,}$ is the volumetric sediment concentration of a specific type (k), L is the vector that defines sediment concentration of each type, F is the matrix of coefficients that define each sediment type, and t is the time.

Sediment accumulation relies on (i) basin geometry and tectonics (Bajpai et al. 2001) (ii) erosion and volume of sediment transported (Cheng, et al. 2018), (iii) prevailing accommodation.

Based on Cheng et al. (2018), sediment accumulation over a period (A_r) is:

$$A_r = V_{er} - V_{es} \qquad (10)$$

$V_{es,}$ is the total volume of sediments that may escapes from the basin. V_{er} is the total volume of sediments eroded into the basin. $V_{er} = A_{er} \text{ x } R_{er} \text{ x } t$; where A_{er} is the average erosion area, R_{er} is the average erosion rate, and t, time.

Because source position for the sediment accumulation process is areal, the volume of sediments accumulated in a specific layer (k) in the basin; excluding porosity, is expressed as:

$$A_r = \sum_{k=1}^{n} A_{rk} \qquad (11)$$

Taking into account the impact of porosity (ϕ) in this process, the equation for the sediment accumulation is:

$$A_r = \sum_{k=1}^{n} [(1 - \phi_0 * e^{-c*z_k}) \; X \; V_{observed_k} \qquad (12)$$

Where; $V_{observedk}$ is the volume of sediment and porosity observed in a specific layer (k), ϕ_0 is the surface porosity, c is the porosity-depth coefficient (after Sclater & Christie, 1980), and Z_k is the average depth of the layer k.

Boundary Conditions for Forward Stratigraphic Simulation

~~A realistic~~Realistic reproduction of stratigraphic patterns in the ~~study~~model area ~~will require~~requires input parameters ~~or~~ (initial

conditions), such as~~: hypothetical~~ paleo-topography, sea-level curves, sediment source location, and distribution curve, tectonic event maps (~~i.e.~~ subsidence and uplift), and sediment mix velocity. The application of these input parameters in GPM™~~,~~ and their ~~influence~~ impact on the resultant stratigraphic framework ~~are discussed~~is below.

Hypothetical Paleo-Surface: The hypothetical paleo-topographic ~~surface, on which~~for the stratigraphic simulation ~~evolves was~~ ~~inferred~~is from the seismic ~~section. This is done with~~data (Figure 3), using the assumption that the present day stratigraphic surface (~~i.e.~~ paleo shoreline in Figure ~~3a~~4a) occurred as a result of basin filling ~~through different~~over geological ~~periods~~time. Since the ~~hypothetical topography generated~~ surface obtained from the seismic section have undergone various phases of subsidence and uplifts, it is significant to note that the paleo topographic surface used in this work does not ~~present~~represent an accurate description of the basin at the period of sediment deposition~~. To obtain~~; thus presenting another level of uncertainty in the simulation. To derive an appropriate paleo-topographic for this task, ~~,~~ five paleo topographic surfaces (TPr) were generated, by adding or subtracting elevations from the inferred paleo topographic surface (see Figure 4g) using the equation:

$$TPr = Sbs + EM \qquad (13)$$

where, Sbs is the base surface scenario (in this instance, scenario 6), and EM an elevation below and above the base surface. ~~Paleo-~~

The paleo-topographic surface in scenario 3 (figure 4d) ~~was~~is selected~~,~~ because it ~~controlled the development of~~ produced a stratigraphic sequences that fit the ~~conceptual knowledge of~~ depositional ~~framework as observed in~~patterns interpreted from the seismic section (Figure 5d).

Sediment Source Location: Based on regional well correlations in ~~previous studies (e.g.~~ Kieft et al.

2011~~),~~ and seismic interpretation of the basin structure, the sediment entry point ~~was~~is placed in the north-eastern section of the hypothetical paleo-topography~~. Since the~~ surface. The exact sediment entry point ~~is not known,~~ ~~multiple~~into this basin is unknown, so three entry points were placed at a 4 km radius around the primary location ~~in~~ (Figure 3c~~), in order~~) to capture possible sediment source locations~~.~~ in the model area. The source position is ~~characterised by~~a positive ~~integers (i.e.~~ integer (values greater than zero) to enable ~~fluid flow~~sediment movement to other parts of the ~~simulation~~topographic surface.

Sea Level: ~~Sea~~ The sea level ~~variation was inferred~~curve is deduced from published studies and facies description in shallow marine depositional environments (e.g. Winterer and Bosellini, 1981). To ~~attain stability in the simulator, we assumed a~~ sea level ~~that range between 15 m to 45 m; averaging~~was constrained 30 m for short simulation runs~~, e.g.~~ (5000 to 20000 years~~. The sea level was~~), but varied with the increasing duration of the simulation (~~illustrated in~~ see Table 2). The peak sea-level in the simulation ~~represents~~depicts the maximum flooding surface (Figure 5d), and therefore the inferred sequence boundary in the geological process model.

Diffusion and Tectonic Event Rates: The sediment mix proportion, diffusion rate, and tectonic event functions ~~were inferred~~are from ~~previous~~ studies ~~(e.g.~~such as Walter, (1978~~;~~), Winterer and Bosellini, (1981~~,~~), and Burges et al., (2008). The diffusion and tectonic event rates ~~are~~were increased or reduced to produce a stratigraphic model that fit our knowledge of ~~the~~ basin evolution~~. A key criteria for selecting parameters is their capacity to produce stratigraphic outputs that depict depositional scenarios~~ in the study area. For example, in scenario 1 (Figure 6a), the early stages of clinoform development show resemblance to interpreted trends in the seismic section (**Figure 3b**). ~~As a result, input figures that were higher and lesser than those used in generating scenario 1 were generated to serve as the simulation parameters for the twenty scenarios. In scenario 1,~~ The process commenced with a diffusion coefficient of 8 m2/a ~~was used to produce a realistic clinoform build-up, so the figure was~~, but it varied ~~with +/- 5~~at each scenario to obtain ~~figures that could~~diffusion coefficients to improve the model ~~derived in scenario 1. The~~. Excluding the initial topography (~~TP,) was kept constant throughout a simulation, but~~ Figure 4d), input parameters in geological processes such as wave events, steady/unsteady flow, diffusion, and tectonic events ~~use~~used curve functions to provide variations ~~within~~in the simulation.

~~simulation. A sudden change in subsidence rate tends to constrain coarse to medium sediments at proximal distance to source location than in scenarios where the rate of subsidence was made gradual.~~

The ~~influence~~sensitivity of input parameters in the forward stratigraphic simulation is ~~evident whenever~~notable when there is a ~~slight~~ change of value in sediment diffusion, and tectonic rates or dimension of the hypothetical ~~topographic surfaces.~~ topography. For example, a change in sediment source position ~~has a strong impact on~~affects the extent and depth ~~to which~~of sediments ~~are deposited~~deposition in the ~~basin~~simulation. Shifting the source point to the mid-section of the topography (~~i.e.~~ the mid-point of the topography in a basin-ward direction) resulted in the accumulation of distal elements ~~that are~~ identical to turbidite lobe systems. This output is consistent with morphodynamic experiments by de Leeuw et al~~.,~~. (2016~~,~~), where sediment discharge from the basin slope leads to the build-up of basin floor fan units.

Property Classification in Stratigraphic Model

In our opinion, the most appropriate ~~model in this work~~output is the stratigraphic model in **Figure 5d**. This point of view is because, ~~when~~ compared to the depositional description in studies such as Folkestad and Satur (2006); ~~kieft~~Kieft et al~~.,~~. (2011), ~~it produced~~and the seismic interpretation presents a similar stratigraphic sequence ~~that mimics the depositional sequence in the study area. The stratigraphic model was converted into a 3-D format, 20 m x 20 m x 2 m grid cells in order to be used in the property modeling tool in Petrel™. Lithofacies, porosity, and permeability properties are characterized in the stratigraphic using a rule based approach (**Table 3**).~~ . Sediment distribution in each time step of the simulation ~~were~~ was stacked into a single zone framework to attain a simplified model. This ~~was done with the assumption~~ strategy assumes that sedimentary processes that lead to the final build-up of genetic related units within zones of the model will not vary significantly over the simulation period. ~~Property classification in the model was achieved~~The stratigraphic model (**Figure 5d**) was converted into a 3-D format (20 m x 20 m x 2 m grid cells) for the property modeling in Petrel™.

~~with~~ Facies, porosity, and permeability representation in the ~~property calculator tool~~stratigraphic model was done via a rule based approach in Petrel™~~.~~ (see **Table 3**). The classification ~~was~~is driven by depositional depth, geologic flow velocity, and sediment distribution patterns as indicated in **Figure 7**. Lithofacies representation in the stratigraphic model ~~was based~~relied on the sediment grain size pattern~~,~~ and proximity to sediment source. For example, shoreface lithofacies units ~~were characterized using~~ are medium-to-coarse grained sediments, which accumulate at a proximal distance to the sediment source. In contrast, mudstone units ~~were restricted~~ are confined to fine-grained sediments ~~that accumulate at~~ in the distal section of the simulation domain.

Using knowledge from published studies by Kieft et al~~.,~~. (2011~~), porosity and permeability variations in the stratigraphic model were estimated from~~) and wireline-log attributes such as gamma ray, neutron, sonic, and density logs

~~outlined in~~, porosity and permeability variations in the stratigraphic model are estimated (Table 1~~.~~). In previous studies on the Sleipner Øst, and Volve field (~~e.g.~~ Equinor, 2006; Kieft et al~~.,~~. 2011), ~~Shoreface~~shoreface deposits ~~were identified to~~ make up the best reservoir units, ~~whilst~~whiles lagoonal deposits formed the worst reservoir units. ~~Using~~With this ~~as~~ guide, shoreface sandstone units and mudstone/shale units in the forward stratigraphic model ~~were characterized as~~are best and worst reservoir units respectively. The porosity and permeability values in Table 4 ~~were derived~~are from equations in Statoil's petrophysical report of the Volve field (Equinor, 2016):

$$\varnothing_{er} = \varnothing_{D} + \alpha \, . \, (NPHI - \varnothing_{D}) + \beta\cancel{;} \qquad (14)$$

where $\varnothing_{er}$ is the estimated porosity range, $\varnothing_{D}$ is density porosity, α and β are regression constants; ranging between -0.02 – 0.01 and 0.28 – 0.4 respectively, *NPHI* is neutron porosity. In instances where NPHI values for lithofacies units is not available from the published references, an average of 0.25 was used.

~~porosity. In instances where NPHI values for lithofacies units is not available from the published references, an average of 0.25 was used.~~

$$KLOGH_{er} = 10^{(2 + 8 * PHIF - 5 * VSH)} \cancel{;} \qquad (15)$$

where $KLOGH_{er}$ is the estimated permeability range, *VSH* is the volume of clay/shale in the lithofacies unit, and *PHIF*, the fractured porosity. The *VSH* range between 0.01 – 0.12 for the shoreface units, and 0.78 – 0.88 for lagoonal deposits.

~~for the shoreface units, and 0.78 – 0.88 for lagoonal deposits.~~

Property Modeling in Petrel™

The workflow (**Figure 2b**) used for subsurface property ~~(e.g. lithofacies, and petrophysical)~~ modeling in Petrel™ is ~~extended~~ applied to represent lithofacies, porosity, and permeability properties in the ~~forward~~ stratigraphic model. These processes ~~include~~involve:

~~1.~~ Structure ~~modelling:~~ modeling: identified faults within the study area are ~~modelled~~ modeled together with interpreted surfaces from seismic and well ~~data~~correlation to generate the main structural framework, within which the ~~entire~~ property model ~~will be~~is built. ~~The procedures involve modification of~~ Here, fault pillars and connecting fault bodies are linked to ~~one another to attain~~obtain the kind of fault framework

(1) interpreted from the seismic ~~and core~~ data.

~~(2)~~ Pillar gridding: building a “grid skeleton” ~~that is~~ made up of a top, middle and base architectures. Typically,

(2) pillars join corresponding corners of every grid cell of the adjacent grid to form the foundation for each cell within the model. The prominent orientation of faults (I-direction) within the model area was in

an N-S and NE-SW direction, so the “I-direction” was set to NNE-SSW to capture the general structural description of the area.

~~each cell within the model. The prominent orientation of faults (i.e. I-direction) within the model area generally trends in a N-S and NE-SW direction, so the “I-direction” was set to the NNE-SSW direction to capture the structural description.~~

~~(3)~~ Horizons, Zones, and Vertical Layering: stratigraphic horizons and subdivisions (zones) ~~delineates~~ delineate the geological formation’s boundaries. As stratigraphic horizons are ~~inserted~~introduced into the model grid, the surfaces are trimmed iteratively and modified along faults to correspond with displacements across multiple faults. Vertical layering ~~on the other hand defines~~shows the thicknesses and orientation between the layers of the model. Layers ~~in this context describes~~ refers to significant changes in particle size or sediment composition in a geological formation. Using a vertical layering scheme makes it possible to ~~honour~~honor the fault framework, pillar grid, and horizons ~~that have been derived.~~. A constant cell ~~thicknesses~~thickness of 1 m ~~across~~is used in the model ~~was defined~~ to control the vertical scale~~, in~~

(3) ~~which subsurface properties such as~~ of lithofacies, porosity, and permeability ~~attributes are modelled.~~modeling.

~~(4)~~ Upscaling: involves the ~~substation~~substitution of ~~fine~~smaller grid cells with coarser grid cells. ~~This~~Here, log data is ~~done~~transformed from 1-dimensional to ~~assign~~ ~~property values~~a 3-dimensional framework to ~~cells in order to~~ evaluate which discrete value suits ~~each a~~ selected data point~~.~~

(4) in the model. One advantage of the upscaling procedure is to make the modeling process faster.

Porosity and Permeability Modeling

The Volve field porosity and permeability model ~~that was built by~~ from Equinor ~~for their operations in the Volve field was~~ are adopted as the base (reference) model. The model~~. The model~~, which ~~cover an area of~~covers 17.9 km^2 was generated with the reservoir management software (RMS), developed by Irap and Roxar (Emerson™). The petrophysical -model has a grid dimension of 108 m x 100 m x 63 m~~,~~ and was compressed by 75.27% of cell size from an approximated cell size of 143 m x 133 m x 84 m. To achieve a comparable model resolution as the Volve field porosity and permeability model, the forward stratigraphic output, which had an initial resolution of 90 m x 78 m x 45 m ~~was~~, is upscaled to a grid of 107 m x 99 m x 63 m. ~~Two~~Variograms being a critical aspect of this work, we submit two options ~~were explored with respect~~ to ~~the use of~~extrapolate variogram parameters ~~derived~~ from the forward ~~model~~stratigraphic-based ~~synthetic wells.~~porosity and permeability models. In Option -1 ~~was to assign~~, the porosity and permeability values were assigned to the synthetic lithofacies wells that ~~correspond to~~correlate with known facies-~~associations as indicated in~~association in the study area (see **Table 4**~~.~~). The ~~synthetic~~pseudo wells ~~with~~comprising porosity and permeability ~~data~~ are ~~placed~~ situated in-between ~~known data~~well locations to guide porosity and permeability ~~property distribution~~simulation in the model.- For -option -2, -the- best-fit -forward -stratigraphic -model ~~-was populated with~~ changes by assigning porosity~~,~~ and permeability ~~attributes~~attribute using the ~~major~~general stratigraphic orientation captured in the seismic data (~~i.e.~~ NE-SW; 240~~º) to control property distribution trends.~~º). Porosity and permeability ~~were populated into the modelby using the property modeling process in Petrel™. Porosity and permeability synthetic~~ pseudo (synthetic) logs ~~are~~ were then extracted from the forward stratigraphic output to build the porosity and permeability models (**Figure 8**).

Porosity modeling is through normal distribution, whiles the permeability models were produced using a log-normal distribution and the corresponding porosity property for collocated co-kriging.

~~Taking into account the possibility~~Considering that vertical trends in options 1 and 2 will be similar ~~in~~within a sampled interval, ~~it is our opinion that~~ option 2 ~~will provide~~presented a viable 3-D representation of property variations in the major and minor directions of the forward stratigraphic model. Ten synthetic wells (SW), ranging between 80 m and ~~a~~ 120 m in total depth (TD~~) were~~), are positioned in the forward model to capture the vertical distribution of porosity-permeability at different sections of the forward stratigraphic ~~model.~~-based models.

The ~~forward-based~~ synthetic wells (**Figure 9 c**) with porosity and permeability ~~logs~~data were upscaled ~~to populate~~, and distributed into the original structural model using the sequential Gaussian simulation method. ~~Here, the~~ The synthetic wells derived from the stratigraphic model ~~is to provide~~served as an additional ~~well data~~control for ~~use in a traditional~~porosity and permeability modeling ~~workflow as was~~ in the ~~case in the building of original~~ Volve ~~model. Considering~~field. Because the ~~advantages of~~ variogram-based modeling ~~in relation to~~ approach is efficient in subsurface data conditioning, ~~the~~this idea ~~was~~presents an opportunity to get more wells ~~into the model grid~~ at no additional cost to control porosity and permeability distribution. ~~Upscaling the synthetic well data in this context is to "transform" the data from 1-D into a 3-D framework to build the property model. Using the same structural model was to attain a comparable framework for evaluating the modeling outputs.~~

The variogram model (**Figure 10**~~),~~) of dominant lithofacies units in the ~~formation~~stratigraphic model served as a guide in ~~the estimation of~~ estimating variogram parameters ~~from the forward model. A~~for porosity and permeability modeling. The variogram has major and minor range of 1400 m and 400 m respectively, and an average sill value of 0.75 ~~derived from forward stratigraphic-based synthetic wells were used to populate porosity and permeability properties in the model. Porosity models were derived with a normal distribution, whilst the permeability models were produced using a log-normal distribution and the corresponding porosity property for collocated co-kriging. Out of~~ . Six out of fifty model realizations~~, six realizations~~ that ~~showed~~show some similarity to the original ~~petrophysical~~porosity and permeability model ~~are presented~~ formed the basis of our analysis (**Figure 11**). ~~This~~The selection of six realizations was ~~accomplished through~~on a visual and statistical comparison of zones in the original ~~Volve field model,~~ Volve field model and the stratigraphic-based porosity/permeability model. The statistical approach involved summary statistics from the reference model and the stratigraphic-based porosity/permeability ~~models. The statistical approach involved a comparison of summary statistics from the original Volve model, and the porosity/permeability model generated through forward stratigraphic modeling. The~~ model. In contrast, the visual ~~comparison on~~

~~the other hand looked~~ ~~at how~~evaluation compared the geological ~~realistic the output is, and if it conforms with our conceptual idea of the Volve field~~realism of forward stratigraphic-based realizations to the base model. ~~model.~~

Results

The stratigraphic model in stage 4 (**Figure 5d iv**) shows the final geometry after 700,~~-~~000 years of simulation time. ~~Initial~~ The initial stratigraphic simulation produced a progradation sequence with foreset-like features (**Figure 5d i**~~). A~~) and a sequence boundary, which ~~indicates the highest sea level in the model~~ separates the initial simulated output from the next prograding phase (**Figure 5d ii**). ~~Initiation of an aggradation~~An aggradational stacking pattern ~~starts,~~commences and becomes prominent in stage 3 (**Figure 5d iii**). These aggradational sequences observed in the forward stratigraphic model are consistent with ~~real-world scenario~~ natural events where sediment supply matchup with accommodation ~~created as a result of the relative~~ due to sea-~~-~~level rise within a geological period (~~e.g.~~ Muto and Steel, 2000; Neal and Abreu, 2009). ~~The diffusion process in GPM™ was used to define the stratigraphic architecture before introducing additional geological processes such as steady flow, unsteady flow, wave events to capture the range of possible depositional styles that have been discussed in published literature (e.g. Folkestad & Satur, 2006; Kieft et al., 2011).~~

~~The impact of the~~Impact of the forward stratigraphic simulation on porosity and permeability representation in the reservoir model ~~was evaluated~~is evident by comparing its outcomes to the Volve field porosity and permeability models by using two synthetic well~~,~~ (VP1 and VP2~~, which were~~); sampled ~~vertically~~ at a 5 m ~~intervals. Considering~~vertical interval. Taking into account the fact that the Volve field petrophysical model (**Figure 11a**) ~~have undergone~~went through various phases of history matching to ~~enhance~~ obtain a model to improve well planning~~,~~ and production strategies ~~in the Volve field~~, it is reasonable to assume that porosity and permeability distribution in the petrophysical model will be geologically realistic and less uncertain. ~~A~~ This view formed the basis for using the porosity and permeability models developed by Equinor as a reference for comparing outputs in the stratigraphic model. **Table 5a** shows an almost good match in porosity ~~was observed in validation wells that penetrate the model realizations;~~ at different intervals in the forward stratigraphic-based models (i.e. R14, R20, R26, R36, R45, and R49 ~~(**Table 5a**).~~). An analysis of the well logs in the model area shows that a large proportion of reservoir porosity is between 0.18 – 0.24. Also, the analysis of the forward stratigraphic-based porosity model is consistent with the porosity range in the Volve field model (see Figure 12 ~~shows the porosity variation (0.18 – 0.24) in some selected~~). ~~realizations. This value (i.e. 0.18 – 0.24) is within the range of porosity estimates in the Volve field~~

~~(Equinor, 2016). In view of the~~ A notable limitation ~~in making variations within a simulation run in GPM™, the forward stratigraphic-based model (FSM) was derived with an~~ with this approach is the assumption that variogram parameters~~,~~ and stratigraphic inclination within zones ~~will remain constant. As a result,~~remained constant throughout the simulation. The difference in permeability attributes between the original ~~petrophysical model, which involve~~ permeability model and the forward stratigraphic-based type is the application of other measured ~~attributes within the stratigraphic zone was not considered~~parameters in the ~~forward stratigraphic modeling-based permeability~~ original model~~, hence the major variations noted in~~ (**Table 5b~~.~~**). Typically, a petrophysical model like the Sleipner Øst and Volve field model will ~~take into account~~factor in other ~~sources of data. For example, data from a~~ datasets such as special core analysis (SCAL) ~~will improve the~~and level of cementation, which enhances reservoir petrophysics assessment. ~~Considering~~Bearing in mind that the ~~FSM approach~~forward stratigraphic model did not involve ~~these~~some of this additional information from the ~~formation,~~ reservoir, it is ~~reasonable~~ practicable to suggest that results obtained in the forward stratigraphic-based porosity and permeability models have ~~been~~ adequately conditioned to known subsurface data.

Discussion

Results show the influence of sediment transport rate~~,~~ (or diffusion rate), initial basin topography, and sediment source location on the stratigraphic simulation in ~~the~~in GPM™ ~~software. Similar~~. Compared to ~~other~~ studies ~~(e.g.~~ such as Muto & Steel~~,~~ (2000~~;~~) and Neal & Abreu~~,~~ (2009), we observed that a ~~variations~~variation in sea-level controls the volume of sediment that ~~could be~~ is retained or transported further into the basin~~;~~, therefore controlling the ~~kind of~~resultant stratigraphic sequences ~~that are generated.~~. In ~~a~~ related work ~~by~~, Burges et al. (2008~~), it was established~~) suggest that a sediment-wedge topset width ~~was~~connects directly ~~linked~~ to the initial bathymetry, in which the sediment-wedge structure ~~was formed, as well as~~ develops, and the correlation between sediment supply and accommodation rate. This opinion is in line with observations in this study, where the initial sediment deposit ~~control~~controls the geometry of subsequent ~~phase~~ phases of depositions~~.~~ in the hypothetical basin. The uncertainty of initial conditions used in this work led to the generation of multiple forward stratigraphic scenarios to account for the range of bathymetries that may have influenced sediment transportation to form the present-day ~~Hugin formation.~~ reservoir units in the Volve field.

The simulation produced well-defined sloping depositional surfaces in a stratigraphic architecture (~~i.e.~~ clinoforms) and sequence boundaries that depict ~~the pattern observed~~ patterns seen in the seismic data. ~~Indicated in previous studies, (e.g.~~In their work, Allen and Posamentier~~,~~ (1993~~;~~); Ghandour and Haredy~~,~~ (2019) explained the importance of sequence stratigraphy ~~is vital~~ in ~~the~~lithofacies characterization ~~of lithofacies in~~, and therefore petrophysical property distribution in sedimentary systems. ~~Therefore, a reproduction of stratigraphic sequence~~ Also, sediment deposition into a geological basin in the natural order is controlled by mechanical and geochemical processes that modify petrophysical attributes (Warrlich et al. 2010); therefore, using different geological processes and initial conditions to generate depositional scenarios in 3-~~D, using the forward~~

~~stratigraphic modeling approach in GPM™ provide a good~~dimension provides a framework to analyse property variations in a hydrocarbon reservoir. ~~A~~The approach produces a porosity-permeability model ~~matching~~comparable to the original petrophysical model ~~was produced~~ using synthetic porosity and permeability logs from the forward stratigraphic model as input datasets ~~in the sequential Gaussian simulation algorithm.~~. As mentioned ~~previously~~, this ~~exercise~~work did not ~~take into account~~include variations in the layering scheme that develops in different zones of the stratigraphic model. Under this circumstance, ~~we concede that~~ there is a possibility to overestimate and or underestimate porosity and permeability ~~properties as observed~~property in some sampled intervals ~~of~~in the validation wells. ~~In view of this, it is our suggestion~~ Therefore, we suggest that the forward stratigraphic simulation outputs ~~should be applied as~~ such as the example presented in this contribution serve as additional data to understand sediment distribution patterns~~,~~ and associated vertical and horizontal petrophysical trends in the depositional environment ~~than using its outputs~~, and not as ~~an~~ absolute conditioning data in subsurface property modeling.

~~Assumptions~~The assumptions made ~~with respect to~~concerning the type of geological processes~~,~~ and input parameters ~~to use~~ in the stratigraphic simulation certainly differ from what existed during ~~the period of~~sediment deposition. So, applying stratigraphic models that fit a basin~~-~~-scale description to a relatively smaller scale reservoir ~~context~~ presents another ~~degree~~level of uncertainty in the approach ~~used here. For example, in their study,~~. This finding agrees with Burges et al., (2008~~) shows~~), where they indicate that the diffusion geological process simulation fits the description of large~~-~~-scale sediment transportation~~; suggesting~~. This view further buttresses the point that ~~an~~ ~~extrapolation of its outputs~~ integrating forward stratigraphic simulation into a well-scale framework ~~could produce results~~has a high chance of producing outcomes that deviate from the real-world ~~distribution.~~subsurface description. In ~~reality, sediment deposition into a geological basin is also controlled by mechanical and geochemical processes that tend to modify a formations petrophysical attributes (Warrlich et al. 2010). Therefore, using different geological processes and initial conditions to generate depositional scenarios is a reasonable approach. However, based on the approach limitation, which are also discussed~~ line with observations in ~~similar works (e.g.~~ Bertoncello et al. (2013~~;~~); Aas et al. (2014~~;~~); and Huang et al. (2015) ~~caution must be taken~~ in ~~using its~~ relations to limitations in the forward stratigraphic simulation method, it is advisable to use its outputs cautiously in ~~real~~ reservoir modeling; as ~~it~~ such outputs from forward stratigraphic models could lead to an increase in property representation bias~~.~~ in a model.

The correlation between reservoir lithofacies and petrophysics, and its prediction through reservoir models, have been extensively examined in ~~previous~~several studies~~,~~ ~~e.g.~~ (Falivene et al~~. (~~., 2006~~)~~; Hu and Chugunova, ~~(~~2008~~), but~~). Meanwhile, the ~~difference in~~ predicted ~~and~~outputs most often do not depict the actual reservoir character ~~is less understood. This in large part is~~ due to the absence of a realistic 3-D stratigraphic framework to guide reservoir property representation in ~~geocellular~~geological models. ~~It is our opinion that~~The forward stratigraphic modeling ~~methods provide~~method, notwithstanding its limitations, provides reservoir modeling practitioners ~~a better~~an platform to generate subsurface models that reflect the natural variation of reservoir properties.

~~appropriate 3-D lithofacies models to improve petrophysical property prediction in a reservoir, but its outputs should be used cautiously and together with verifiable subsurface patterns from seismic and well datasets.~~

Conclusion

In this paper, ~~spatial data~~variogram parameters from a forward stratigraphic simulation ~~is~~are combined with subsurface data ~~from the Volve field, Norway~~ to constrain porosity and permeability distribution in ~~inter-well regions of~~ the Volve field model ~~area. As~~. The caution~~,~~ for subsurface modeling practitioners is that the ~~forward~~ stratigraphic simulation scenarios presented in this contribution do not ~~ultimately~~ prove that spatial and geometrical data derived from forward stratigraphic ~~modeling can be used as~~

models are absolute input parameters for a real-world reservoir modeling task. Uncertainties in the choice of ~~initial~~ ~~condition~~boundary conditions and processes for the stratigraphic simulation led the variation of input parameters ~~in order~~ to attain a depositional architecture that is geologically realistic and comparable to the stratigraphic correlation suggested in some published studies of the study area. The ~~good~~ match in porosity obtained ~~from~~ by comparing validation wells in the original and stratigraphic-based petrophysical model~~, leads us to the suggestion~~ indicates that ~~an integration of~~combining variogram parameters from well data and forward stratigraphic simulation outputs will improve property prediction in inter-well zones. This suggestion ~~is supported by~~supports the idea that more conditioning data (well data) will increase the chance of producing realistic property distribution in the model area. ~~In addition, this~~This work also made some key findings:

1. For ~~a~~ specific ~~application of forward~~ stratigraphic ~~modeling~~simulation in GPM™ and a range of model parameters, ~~the process of~~ sediment transportation and deposition is ~~influenced by~~ based on diffusion rate~~,~~ and proximity to sediment source. This opinion is consistent with several published works on sequence ~~stacking~~stratigraphy and or system tracts in shallow marine settings~~, but~~. However, further work with different stratigraphic modeling simulators could ~~be useful in mitigating~~mitigate some of the challenges faced in this work.

2. ~~A geologically viable 3-D~~A lithofacies distribution that is consistent with previous studies was produced in the ~~shallow marine Hugin formation was achieved, which is~~ stratigraphic model. This position is evident in scenarios where sediment distribution vertically matches with lithofacies variation in a sampled interval in an actual well log.

Geologically feasible stratigraphic patterns generated in the forward stratigraphic model provide additional confidence in the representation of lithofacies, and therefore porosity and permeability property variations in the depositional setting under study. The resultant forward stratigraphic-based porosity and permeability model suggests that forward stratigraphic simulation outputs can be integrated into classical modeling workflows to improve subsurface property modeling and well planning strategies.

~~modeling workflows to improve subsurface property modeling , and well planning strategies.~~

Data and Code Availability

The datasets ~~used in~~for this work ~~was obtained~~are from Equinor on their operations in Volve field ~~operations~~, Norway. ~~This~~

The data include~~:~~ 24 suits of well logs, and 3-D reservoir models in Eclipse and RMS formats. The data, models (eclipse and RMS formats), and the rule-based calculation script to generate lithofacies and porosity/permeability proportions are archived on Zenodo as Otoo & Hodgetts, (2020).

~~proportions are archived on Zenodo as Otoo & Hodgetts, (2020).~~

GPM™ Software

The ~~version~~ (2019.1) version of GPM™ software was used in completing this work after an initial 2018.1 version. Available on: ~~https://www.software.slb.com/products/gpm.~~ https://www.software.slb.com/products/gpm. The software license and code used in the GPM™ cannot be provided, because Schlumberger does not allow the code for its software to be shared in publications.

Model Availability in Petrel™

The work started in Petrel™ software (2017.1~~)~~), but it was ~~initially used for the task, but~~ completed with Petrel™ software (2019.1~~);~~). The software is available on: https~~://www.software.slb.com/products/petrel.~~://www.software.slb.com/products/petrel. The software ~~run~~runs on a ~~windows~~Windows PC with the following specifications: Processor; Intel Xeon CPU E5-1620 v3 @3.5GHz 4 cores-8 threads, Memory; 64 GB RAM. The computer should be high end, because a lot of processing time is required ~~to execute~~a for the task. The forward stratigraphic models are ~~achieved~~ in Zenodo as Otoo & Hodgetts, (2020).

Author Contribution

Daniel Otoo designed the model workflow, conducted the simulation using the GPM^{TM} software, and evaluated the results. David Hodgetts converted the Volve field data into Petrel compactible format for easy integration with outputs from the forward stratigraphic simulation.

~~easy integration with outputs from the stratigraphic simulation.~~

Acknowledgement

Thanks to Equinor for making available the Volve field dataset. Also, thanks to Schlumberger for providing us with the GPM^{TM} software license. A special thanks to ~~Schlumberger for providing the software, and~~ Mostfa Legri (Schlumberger) for his technical support in the use of GPM^{TM}. Finally, to the Ghana National Petroleum Corporation (GNPC) for sponsoring this research.

References

Aas, T., Basani, R., Howell, J. & Hansen, E.: Forward modeling as a method for predicting the distribution of deep-marine sands: an example from the Peira Cava sub-basin. The geologic society, 387(1), 247-269, doi:10.1144/SP387.9, 2014.

~~marine sands: an example from the Peira Cava sub-basin. The geologic society, 387(1), 247-269, doi:10.1144/SP387.9, 2014.~~

Allen, G. P. and Posamentier, H. W.: Sequence stratigraphy and facies model of an incised valley fill; the Gironde Estuary, France. Journal of Sedimentary Research; 63 (3), 378–391, doi:/10.1306/D4267B09-2B26-11D7-8648000102C1865D, 1993.

~~Estuary, France. Journal of Sedimentary Research; 63 (3), 378–391, doi:/10.1306/D4267B09-2B26-11D7-8648000102C1865D, 1993.~~

Bajpai, V.N., Saha Soy, T.K., Tandon, S.K.: Subsurface sediment accumulation patterns and their relationships with tectonic lineaments in the semi-arid Luni river basin, Rajasthan, Western India. Journal of Arid Environments, 48(4); 603-621, 2001.

Bertoncello, A., Sun, T., Li, H., Mariethoz, G., & Caers, J.: Conditioning Surface-Based Geological Models to Well and Thickness Data. International Association of Mathematical Geoscience, 45, 873-893, doi: 10.1007/s11004-013-9455-4, 2013.

~~Well and Thickness Data. International Association of Mathematical Geoscience, 45, 873-893, doi: 10.1007/s11004-013-9455-4, 2013.~~

Burges, P.M., Steel, R.J., & Granjeon, D.: Stratigraphic Forward Modeling of Basin-Margin Clinoform Systems: Implications for Controls on Topset and Shelf Width and Timing of Formation of Shelf-Edge deltas. Recent advances in models of siliciclastic shallow-marine stratigraphy. SEPM (Society for Sedimentary Geology) Special Publication, vol. 90, SEPM (Society for Sedimentary Geology), 35-45, 2008.~~Recent~~

~~advances in models of siliciclastic shallow-marine stratigraphy. SEPM (Society for Sedimentary Geology) Special Publication, vol. 90, SEPM (Society for Sedimentary Geology), 35-45, 2008.~~

Caers, J., & Zhang, T.: Multiple-point geostatistics: a quantitative vehicle for integrating geologic analogs into multiple reservoir models, in Grammer, G. M., Harris, P. M., and Eberli, G. P., eds., Integration of outcrop and modern analogs in reservoir modeling. Am. Assoc. Petrol. Geol. Memoir, 384–394, 2004.

~~multiple reservoir models, in Grammer, G.~~ Cheng, F., Garzione, C., Jolivet, M., Guo, Z., Zhang, D., & Zhang, C.: A New Sediment Accumulation Model of Cenozoic Depositional Ages From the Qaidam Basin, Tibetan Plateau. Journal of Geophysical Research; Earth Surface. 123, 3101-3121, 2018

~~M., Harris, P. M., and Eberli, G. P., eds., Integration of outcrop and modern analogs in reservoir modeling. Am. Assoc. Petrol. Geol. Memoir, 384–394, 2004.~~

Cockings, J.H., Kessler, L.G., Mazza, T.A., & Riley, L.A.: Bathonian to mid-Oxfordian Sequence Stratigraphy of the South Viking Graben, North Sea. Geological Society, London, Special publications, 67, 65–105, doi:10.1144/GSL.SP.1992.067.01.04, 1992.

~~the South Viking Graben, North Sea. Geological Society, London, Special publications, 67, 65–105, doi:10.1144/GSL.SP.1992.067.01.04, 1992.~~

Dade, W.B. & Friend, P.F.: Grain Size, Sediment Transport Regime, and Channel Slope in Alluvial Rivers. The Journal of Geology, 106(6), 661-676, 1998.

Deutsch, C. & Journel, A.: GSLIB. Geostatistical software library and user's guide. Geological magazine, 136(1), 83-108, doi:10.2307/1270548, 1999.

~~83-108, doi:10.2307/1270548, 1999.~~

De Leeuw, J., Eggenhuisen, J.T., & Cartigny, M.J.B.: Morphodynamics of submarine channel inception -revealed by new experimental approach. Nature Communication, 7, 10886, 2016.

Dubrule, -O.: -Geostatistics in -Petroleum Geology. -American -Association of -Petroleum Geologist, -38, 27-101, doi:10.1306/CE3823, 1998.

Falivene, O., Arbues, P., Gardiner, A., & Pickup, G.E.: Best practice stochastic facies modeling from a channel-fill turbidite sandstone analog (the Quarry outcrop, Eocene Ainsa basin, northeast Spain. American Association of Petroleum Geologist, 90(7), 1003-1029, doi:10.1306/02070605112, 2006.

~~Petroleum Geologist, 90(7), 1003-1029, doi:10.1306/02070605112, 2006.~~

Folkestad, A., & Satur, N.: Regressive and transgressive cycles in a rift-basin: Depositional model and sedimentary partitioning of the Middle Jurassic Hugin Formation, Southern Viking Graben, North Sea. Sedimentary Geology. 207, 1-21, doi:10.1016/j.sedgeo.2008.03.006, 2008.

~~207, 1-21, doi:10.1016/j.sedgeo.2008.03.006, 2008.~~

Ghandour, I.M. and Haredy, R.A.: Facies Analysis and Sequence Stratigraphy of Al-Kharrar Lagoon Coastal Sediments, Rabigh Area, Saudi Arabia: Impact of Sea-Level and Climate Changes on Coastal Evolution. ~~Arabian~~Arabian Journal for Science and Engineering, 44(1), 505-520, 2019.

~~Journal for Science and Engineering, 44(1), 505-520, 2019.~~

Hassanpour, M., Pyrcz, M. & Deutsch, C.: Improved geostatistical models of inclined heterolithic strata for McMurray formation, Canada. AAPG Bulletin, 97(7), 1209-1224, doi:10.1306/01021312054, 2013.

Hodgetts, D.D., Drinkwater, N.D., Hodgson, J., Kavanagh, J., Flint, S.S., Keogh, K.J. and Howell, J.A.: Three-dimensional geological models from outcrop data using digital data collection techniques: an example from the Tanqua Karoo depocenter, South Africa. Geological Society, London, v. 171 (4), 57–75, doi:10.1144/GSL.SP.2004.239.01.05, 2004.

~~Tanqua Karoo depocenter, South Africa. Geological Society, London, v. 171 (4), 57–75, doi:10.1144/GSL.SP.2004.239.01.05, 2004.~~

Hu, L.Y., and Chugunova, T.: Multiple-point geostatistics for modeling subsurface heterogeneity: A comprehensive review. Water Resource Research, 44 (11), 1-14, doi:10.1029/2008WR006993, 2008.

Huang, X., Griffiths, C. & Liu, J.: Recent development in stratigraphic forward modeling and its application in petroleum exploration. Australian journal of Earth science, 62(8), 903-919, doi:10.1080/081200991125389, 2015.

Husmo, T. & Hamar, G.P. & Høiland, O. & Johannessen, E.P. & Rømuld, A. & Spencer, A.M. & Titterton, Rosemary.: Lower and Middle Jurassic. In: The Millennium Atlas: Petroleum Geology of the Central and Northern North Sea, 129-155, 2003.

~~North Sea, 129-155, 2003.~~

Kelkar, M., & Perez, G.: Applied Geostatistics for Reservoir Characterization. Society of Petroleum Engineers. https://www.academia.edu/36293900/Applied_Geostatistics_for_Reservoir_characterization. Accessed 10 September, 2019, 2002.

~~https://www.academia.edu/36293900/Applied Geostatistics for Reservoir characterization. Accessed 10 September, 2019, 2002.~~

Kieft, R.L., Jackson, C.A.-L., Hampson, G.J., and Larsen, E.: Sedimentology and sequence stratigraphy of the Hugin Formation, Quadrant 15, Norwegian sector, South Viking Graben. Geology Society, London, Petroleum Geology Conference Series, 7, 157-176, doi:10.1144/0070157, 2011.

~~Geology Conference Series, 7, 157-176, doi:10.1144/0070157, 2011.~~

Milner, P.S., and Olsen, T.: Predicted distribution of the Hugin Formation reservoir interval in the Sleipner Øst field, South Viking Graben; the testing of a three-dimensional sequence stratigraphic model. In: Gradstein, F.M., Sandvik, K.O., Milton, N.J. (Eds.), Sequence Stratigraphy; Concepts and Applications. Special Publication, Vol 8. Norwegian Petroleum Society, 337-354, 1998.

~~Norwegian Petroleum Society, 337-354, 1998.~~

Muto, T., and Steel, R.J.: The accommodation concept in sequence stratigraphy: Some dimensional problems and possible redefinition. Geology, 130(1), 1-10, 2000.

~~possible redefinition. Geology, 130(1), 1-10, 2000.~~

Neal, J., and Abreu, V.: Sequence stratigraphy hierarchy and the accommodation succession method. Geology, 37(9), 779-782, 2009.

Otoo, D., and Hodgetts, D.: Geological Process Simulation in 3-D Lithofacies Modeling: Application in a Basin Floor Fan Setting. Bulletin of Canadian Petroleum Geology, 67(4), 255-272, 2019.

~~Floor Fan Setting. Bulletin of Canadian Petroleum Geology, 67(4), 255-272, 2019.~~

Otoo, D. & Hodgetts, D. Data citation for a forward stratigraphic-based porosity and permeability model developed for the Volve field, Norway. Dataset. Zenodo. http://doi.org/10.5281/zenodo.3855293, 2020.

~~for the Volve field, Norway. Dataset. Zenodo. http://doi.org/10.5281/zenodo.3855293, 2020.~~

Orellana, N. Cavero, J. Yemez, I. Singh, V. and Sotomayor, J.: Influence of variograms in 3D reservoir-modeling outcomes: An example. The leading edge, 33(8), 890-902, doi:10.1190/tle33080890.1, 2014.

~~outcomes: An example. The leading edge, 33(8), 890-902, doi:10.1190/tle33080890.1, 2014.~~

Patruno, S., and Hansen, W.H.: Clinoforms and clinoform systems: Review and dynamic classification scheme for shorelines, subaqueous deltas, shelf edges and continental margins. Earth-Science Reviews, 185, 202-233, 2018.

Ravasi, M., Vasconcelos, I., Curtis, A. and Kristi, A.: Vector-acoustic reverse time migration of Volve ocean-bottom cable data set without up/down decomposed wavefields. Geophysics 80 (4): 137-150, doi:10.1190/geo2014-0554.1, 2015.

~~bottom cable data set without up/down decomposed wavefields. Geophysics 80 (4): 137-150, doi:10.1190/geo2014-0554.1, 2015.~~

Ringrose., P. & Bentley., M.: Reservoir model design: A practioner's guide. First edition ed. New York: Springer business media B.V. 20-150, 2015.

~~business media B.V. 20-150, 2015.~~

Rijn, L.C., Walstra, D.J.R., Grasmeijer, B., Sutherland, J., Pan, S., & Sierra, J.P.: The predictability of cross-shore bed evolution of sandy beaches at the time scale of storms and seasons using process-based profile models. ~~Coastal~~Coastal engineering, 47(3), 295-327, doi:10.1016/S0378-3839(02)00120-5, 2003.

~~engineering, 47(3), 295-327, doi:10.1016/S0378-3839(02)00120-5, 2003.~~

Schlumberger™ Softwares.: Geological Process Modeling, Petrel™ version 2019.1, Schlumberger, Norway. ~~URL:~~URL: https://www.sdc.oilfield.slb.com/SIS/downloads.aspx, 2019.

~~https://www.sdc.oilfield.slb.com/SIS/downloads.aspx, 2019.~~

Sclater, J.G. & Christie, P.A.F.: Continental stretching: An explanation of the Post-Mid-Cretaceous subsidence of the central North Sea Basin. Journal of Geophysical Research, Solid Earth; 85(7), 3711-3739, 1980.

Singh, V., & Yemez, I., & Sotomayor de la Serna, J.: Integrated 3D reservoir interpretation and modeling: Lessons learned and proposed solutions. The Leading Edge. 32(11), 1340-1353, doi:10.1190/tle32111340.1, 2013.

Skalinski, M., ~~&~~ & Kenter, J.: Carbonate petrophysical rock typing: Integrating geological attributes and petrophysical properties while linking with dynamic behaviour. Geological Society, London, Special Publications. 406 (1), 229-259, 2014.

~~406 (1), 229-259, 2014.~~

Sneider, J.S., de Clarens, P., and Vail, P.R.: Sequence stratigraphy of the Middle and Upper Jurassic, Viking Graben, North Sea. In: Steel, R.J., Felt, V.L., Johannessen, E.P., Mathieu, C. (Eds.), Sequence Stratigraphy on the Northwest European Margin. Special Publication, vol. 5. Norwegian Petroleum Society, 167–198, doi:10.1016/S0928-8937(06)80068-8, 1995.

~~Northwest European Margin. Special Publication, vol. 5. Norwegian Petroleum Society, 167–198, doi:10.1016/S0928-8937(06)80068-8, 1995.~~

Statoil, "Sleipner Øst, Volve Model, Hugin and Skagerrak Formation Petrophysical Evaluation, 2006", Stavanger, Norway. Accessed on: April, 27, 2019. Online: https~~://www.equinor.com/volve-field-data-village-~~ ://www.equinor.com/volve-field-data-village-download.

Strebelle, S., & Levy, M.: Using multiple-point statistics to build geologically realistic reservoir models: the MPS/FDM workflow. Geological Society London, special publication, 309, 67-74, doi:10.1144/SP309.5, 2008.

Tetzlaff, D.M. & Harbaugh, J.W.: Simulating Clastic Sedimentation. New York: Van Nostrand Reinhold, 1989.

Varadi, M., Antonsen, P., Eien, M., & Hager, K.: Jurasic genetic sequence stratigraphy of the Norwegian block 15/5 area, South Viking Graben. In: Gradstein, F. M., Sandvik, K.O., & Milton, N.J., (eds) Sequence Stratigraphy – Concepts and Applications. Norwegian Petroleum Society, Trondheim, special publication, 373-401, 1998.

Vollset, J. and Dore, A.G.: A revised Triassic and Jurassic lithostratigraphic nomenclature for the Norwegian North Sea. NPD Bulletin Oljedirektoratet, 3, 53, 1984.

~~Sea. NPD Bulletin Oljedirektoratet, 3, 53, 1984.~~

~~533~~ Walter C. P.: Relationship between eustacy and stratigraphic sequences of passive margins. GSA Bulletin; 89 (9), ~~534~~ 1389–1403, 1978.

~~535~~ Winterer, L. W., Bosellini, A.: Subsidence and Sedimentation on Jurassic Passive Continental Margin, Southern Alps, Italy. AAPG Bulletin; 65 (3), 394–421, doi: 10.1306/2F9197E2-16CE-11D7-8645000102C1865D, 1981.

~~536 Alps, Italy. AAPG Bulletin; 65 (3), 394–421, doi: 10.1306/2F9197E2-16CE-11D7-8645000102C1865D, 1981.~~

~~537~~ Warrlich, G., Hillgartner, H., Rameil, N., Gittins, J., Mahruqi, I., Johnson, T., Alexander, D., Wassing, B.,

~~538~~ Steenwinkel, M., & Droste, H.: Reservoir characterisation of data-poor fields with regional analogues: a case study from the Lower Shuaiba in the Sultanate of Oman, p. 577, 2010.

~~539 from the Lower Shuaiba in the Sultanate of Oman, p.~~ Zhong, D.: Transport Equation for Suspended Sediments Based on Two-Fluid Model of Solid/Liquid Two-Phase Flows. Journal of Hydraulic Engineering; 137(5), 530-542, doi: 10.1061/(ASCE)HY.1943-7900.0000331, 2011.

~~577, 2010.~~

List of Figures

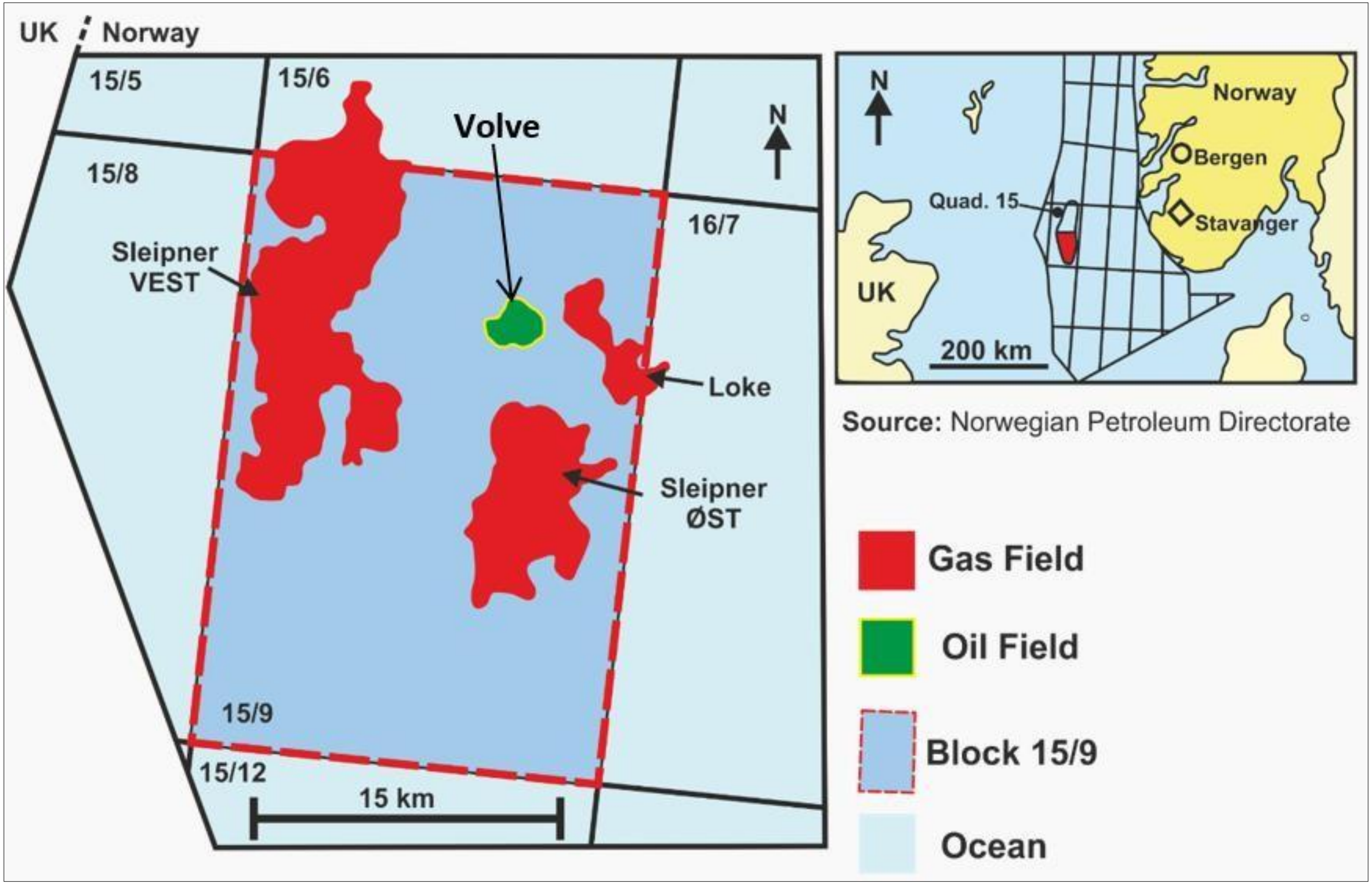

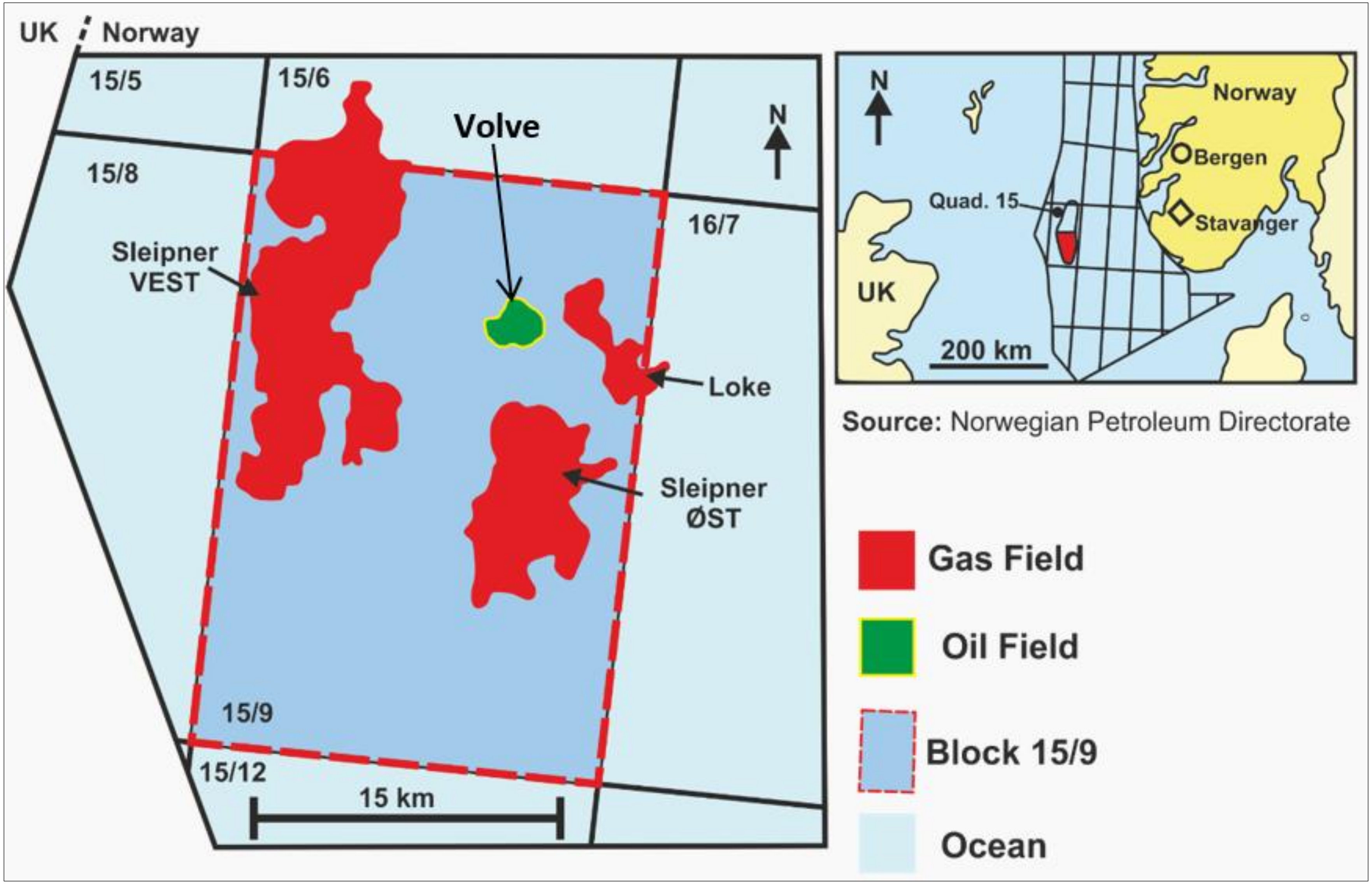

Fig 1. Location map of the Volve field~~,~~; showing gas and oil fields in quadrant 15/9, Norwegian North Sea (~~Adapted~~ from Ravasi et al., 2015).

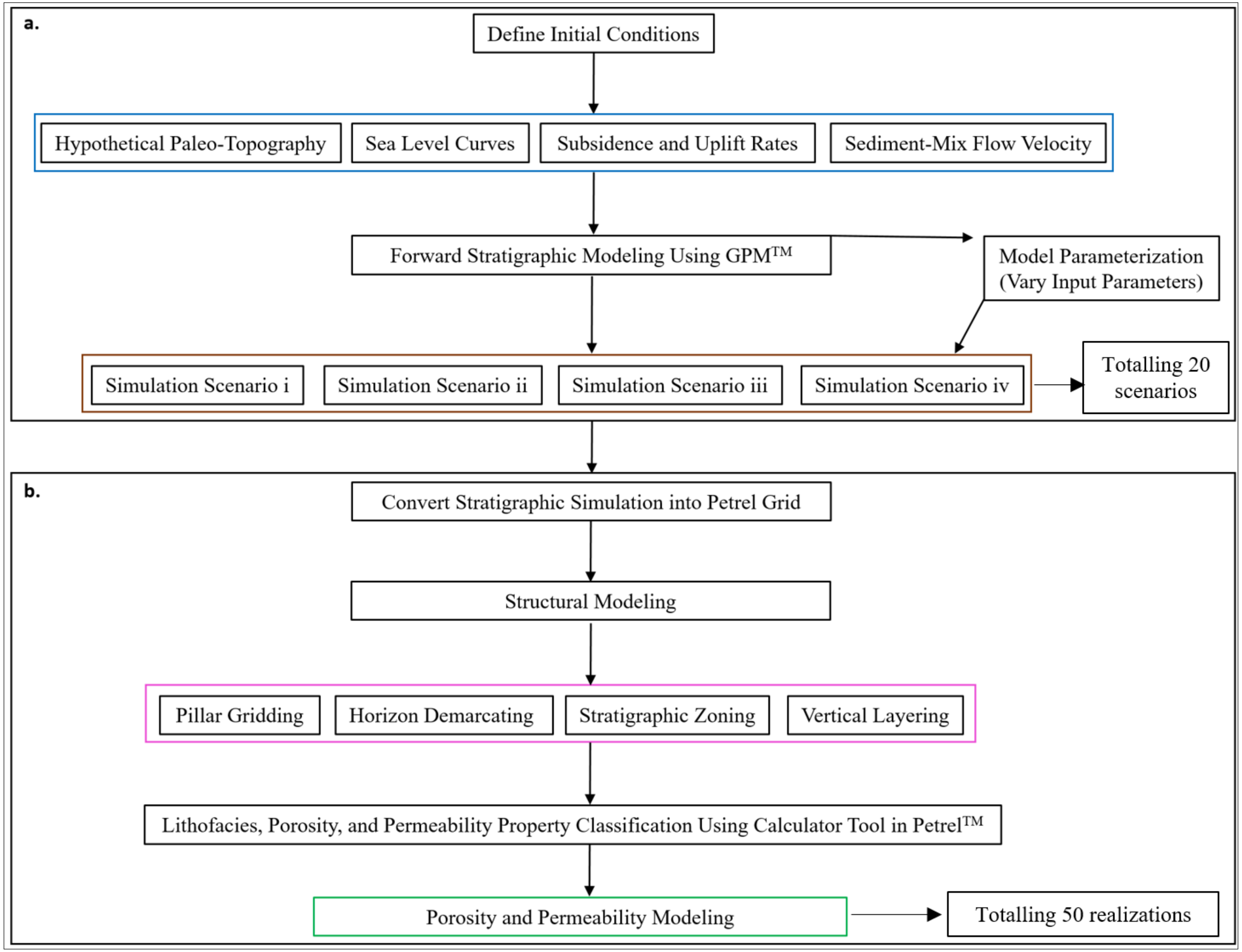
a.
Define Initial Conditions
Hypothetical Paleo-Topography
Sea Level Curves
Subsidence and Uplift Rates
Sediment-Mix Flow Velocity
Forward Stratigraphic Modeling Using GPM™
Model Parameterization (Vary Input Parameters)
Simulation Scenario i
Simulation Scenario ii
Simulation Scenario iii
Simulation Scenario iv
Totalling 20 scenarios
b.
Convert Stratigraphic Simulation into Petrel Grid
Structural Modeling
Pillar Gridding
Horizon Demarcating
Stratigraphic Zoning
Vertical Layering
Lithofacies, Porosity, and Permeability Property Classification Using Calculator Tool in Petrel™
Porosity and Permeability Modeling
Totalling 50 realizations

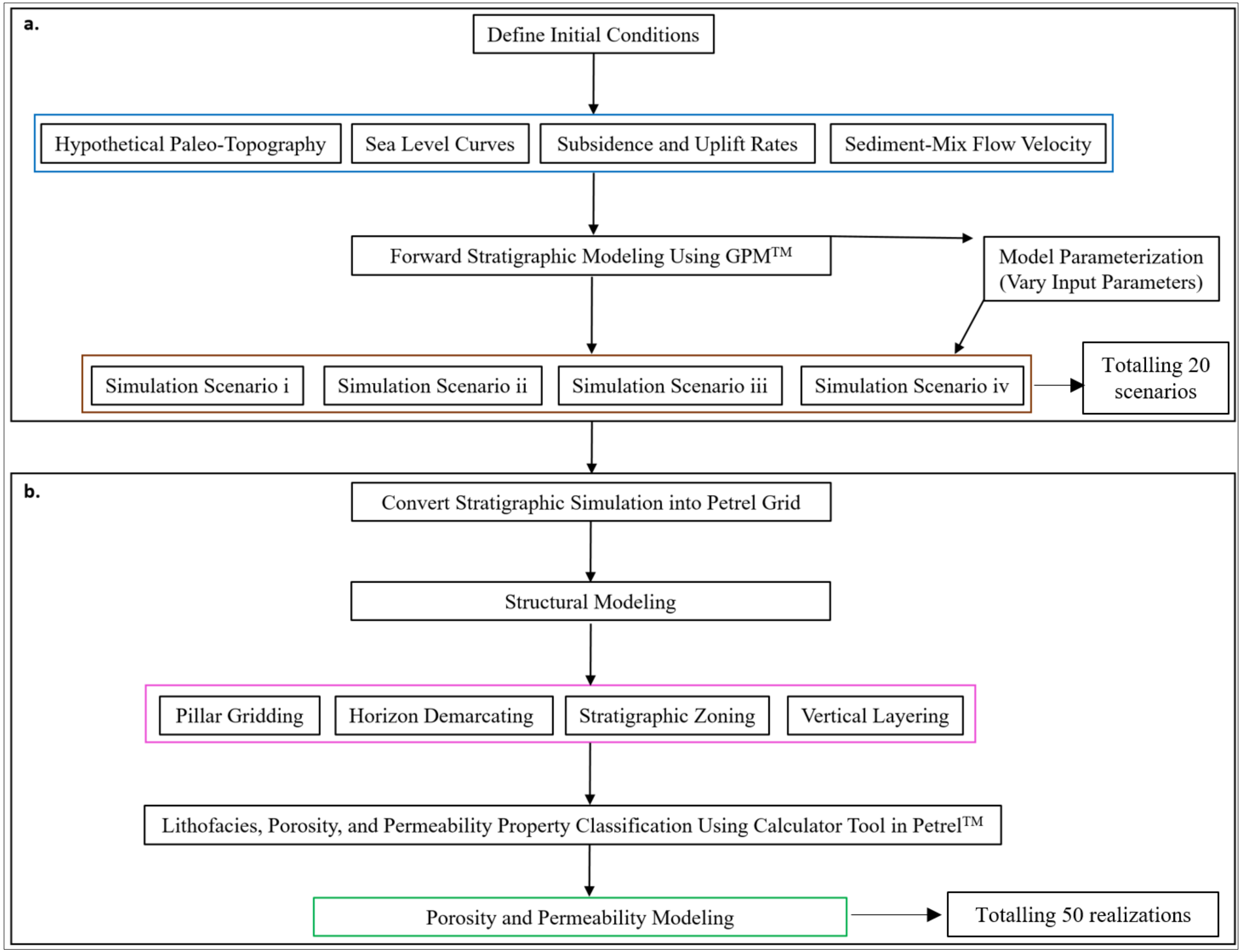
a.
Define Initial Conditions
Hypothetical Paleo-Topography
Sea Level Curves
Subsidence and Uplift Rates
Sediment-Mix Flow Velocity
Forward Stratigraphic Modeling Using GPM™
Model Parameterization (Vary Input Parameters)
Simulation Scenario i
Simulation Scenario ii
Simulation Scenario iii
Simulation Scenario iv
Totalling 20 scenarios
b.
Convert Stratigraphic Simulation into Petrel Grid
Structural Modeling
Pillar Gridding
Horizon Demarcating
Stratigraphic Zoning
Vertical Layering
Lithofacies, Porosity, and Permeability Property Classification Using Calculator Tool in Petrel™
Porosity and Permeability Modeling
Totalling 50 realizations

Fig 2. Schematic workflow of processes involved in this work. a. providing information of ~~initial~~boundary conditions (~~or~~ input parameters) ~~that were~~ used in the forward stratigraphic simulation in GPM™~~,~~; b. ~~demonstrating~~demonstrate how the forward stratigraphic ~~were~~model are converted into a grid that is usable in Petrel™ for porosity and permeability modeling.

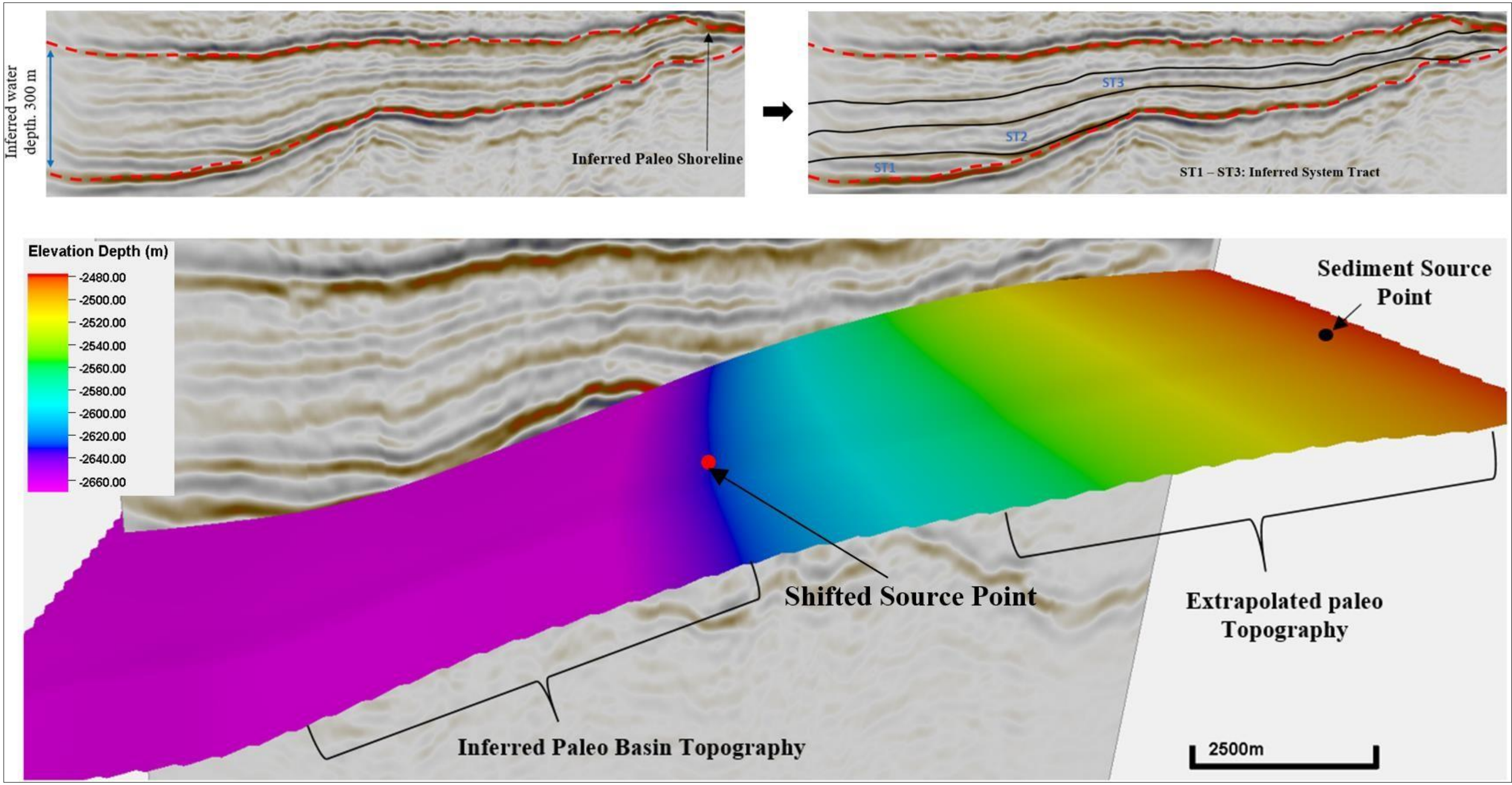
Inferred water depth. 300 m
Inferred Paleo Shoreline
ST3
ST2
ST1
ST1 – ST3: Inferred System Tract
Elevation Depth (m)
-2480.00
-2500.00
-2520.00
-2540.00
-2560.00
-2580.00
-2600.00
-2620.00
-2640.00
-2660.00
Sediment Source Point
Shifted Source Point
Extrapolated paleo Topography
Inferred Paleo Basin Topography
2500m

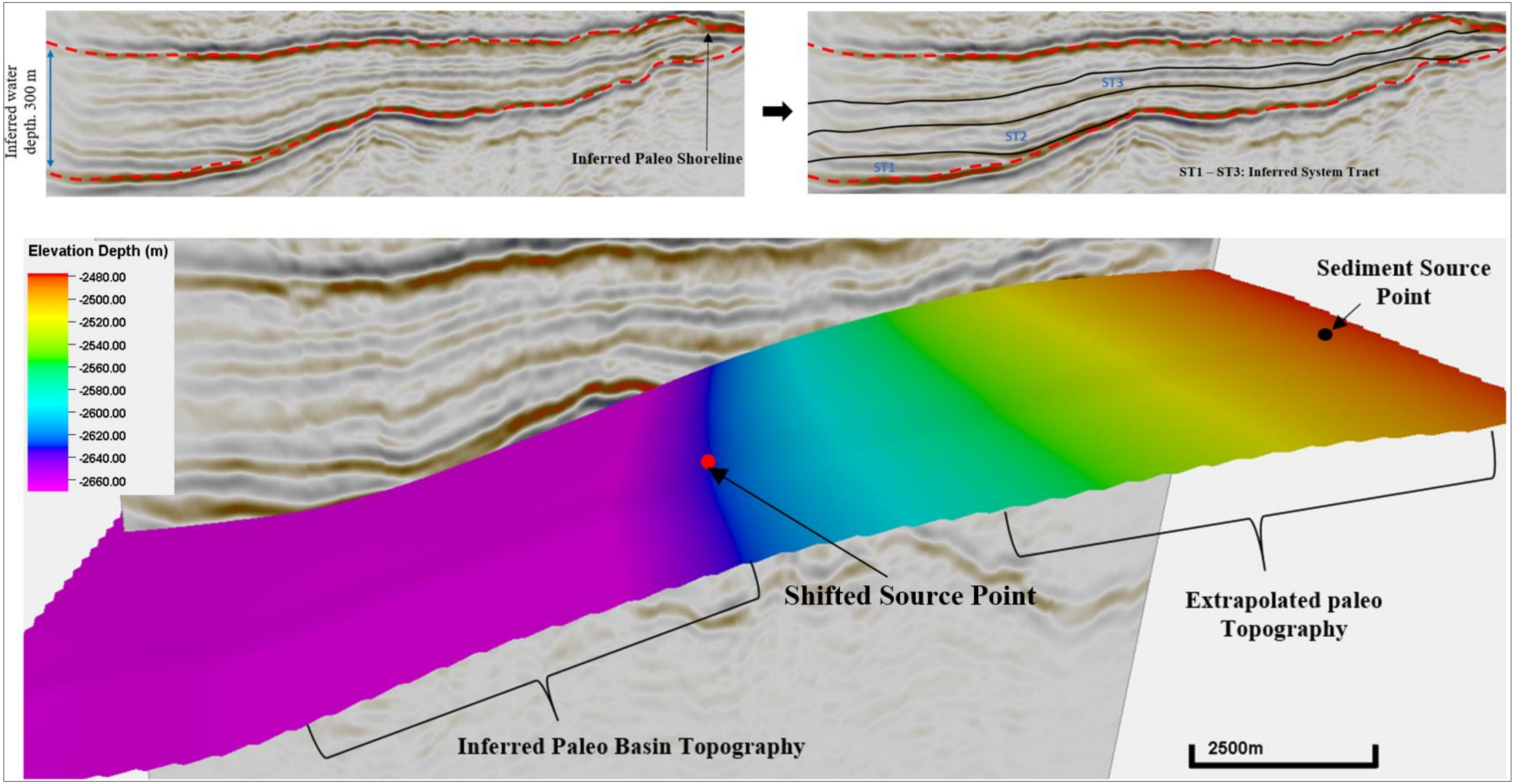

Fig 3. 3-D seismic section of the study area, from which the hypothetical topographic surface ~~was~~is derived for the simulation. The sedimentary entry point into the basin is located in the North Eastern section~~, ~~(based on ~~previous study in the model area (e.g. ~~Kieft et al. 2011).

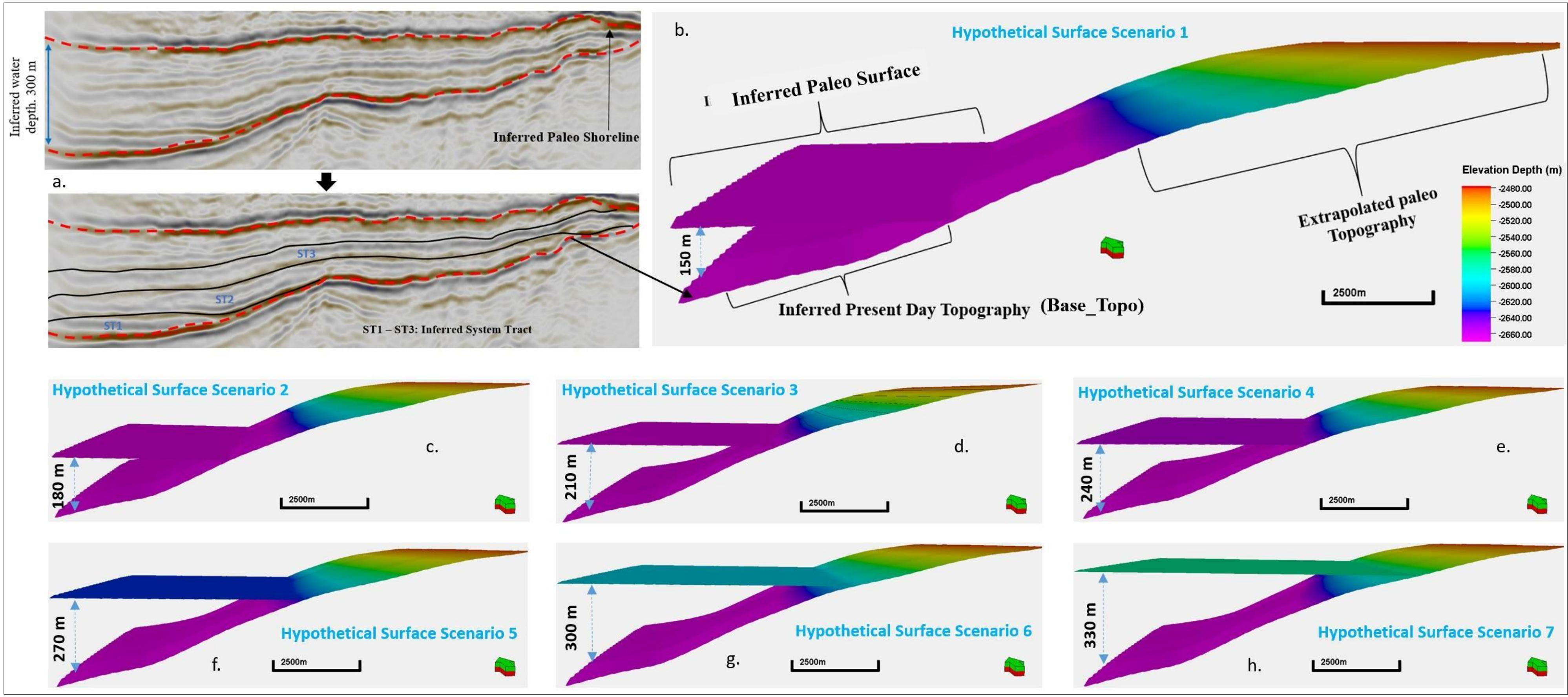
Inferred water depth. 300 m
Inferred Paleo Shoreline
a.
ST3
ST2
ST1
ST1 – ST3: Inferred System Tract
b.
Hypothetical Surface Scenario 1
Inferred Paleo Surface
150 m
Inferred Present Day Topography (Base_Topo)
Extrapolated paleo Topography
Elevation Depth (m)
-2480.00
-2500.00
-2520.00
-2540.00
-2560.00
-2580.00
-2600.00
-2620.00
-2640.00
-2660.00
2500m
Hypothetical Surface Scenario 2
c.
180 m
2500m
Hypothetical Surface Scenario 3
d.
210 m
2500m
Hypothetical Surface Scenario 4
e.
240 m
2500m
270 m
Hypothetical Surface Scenario 5
f.
2500m
300 m
Hypothetical Surface Scenario 6
g.
2500m
330 m
Hypothetical Surface Scenario 7
h.
2500m

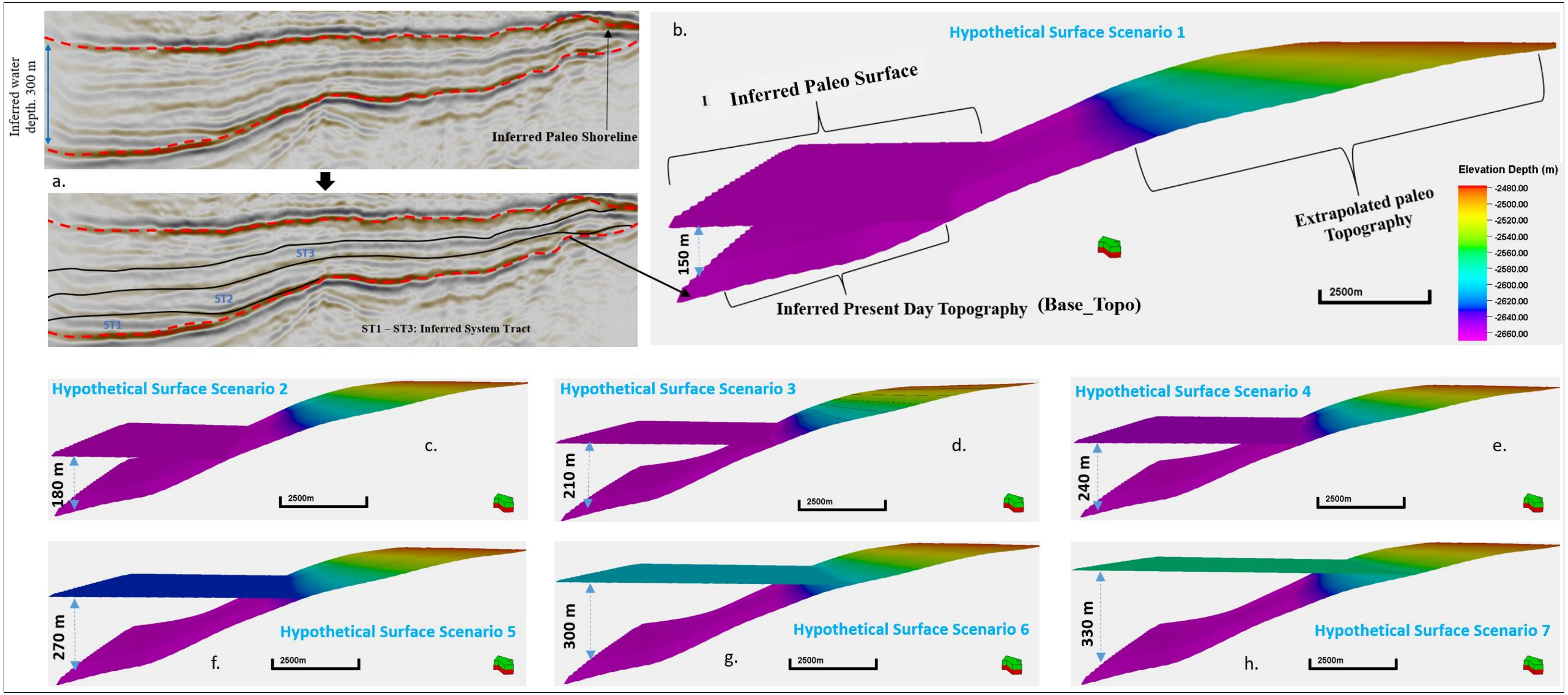

Fig 4. ~~Inferred paleo~~Paleo topographic surface from seismic~~, also~~. Also, illustrating different topographic surface scenarios ~~used in~~that are produced for the simulation.

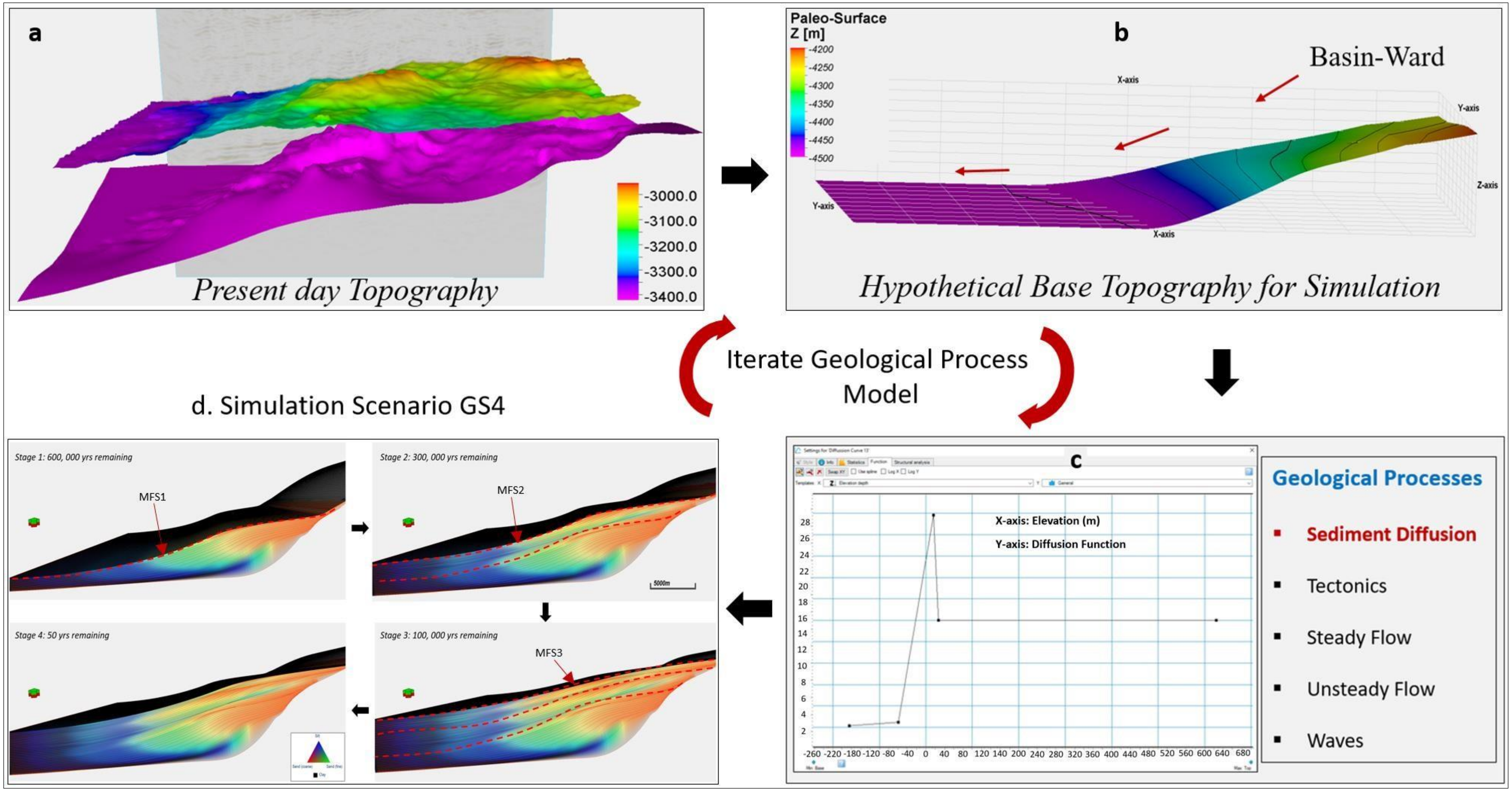
a
-3000.0
-3100.0
-3200.0
-3300.0
-3400.0
Present day Topography
Paleo-Surface
Z [m]
-4200
-4250
-4300
-4350
-4400
-4450
-4500
b
Basin-Ward
X-axis
Y-axis
Z-axis
Hypothetical Base Topography for Simulation
Iterate Geological Process Model
d. Simulation Scenario GS4
Stage 1: 600, 000 yrs remaining
MFS1
Stage 2: 300, 000 yrs remaining
MFS2
5000m
Stage 4: 50 yrs remaining
Stage 3: 100, 000 yrs remaining
MFS3
c
X-axis: Elevation (m)
Y-axis: Diffusion Function
Geological Processes
Sediment Diffusion
Tectonics
Steady Flow
Unsteady Flow
Waves

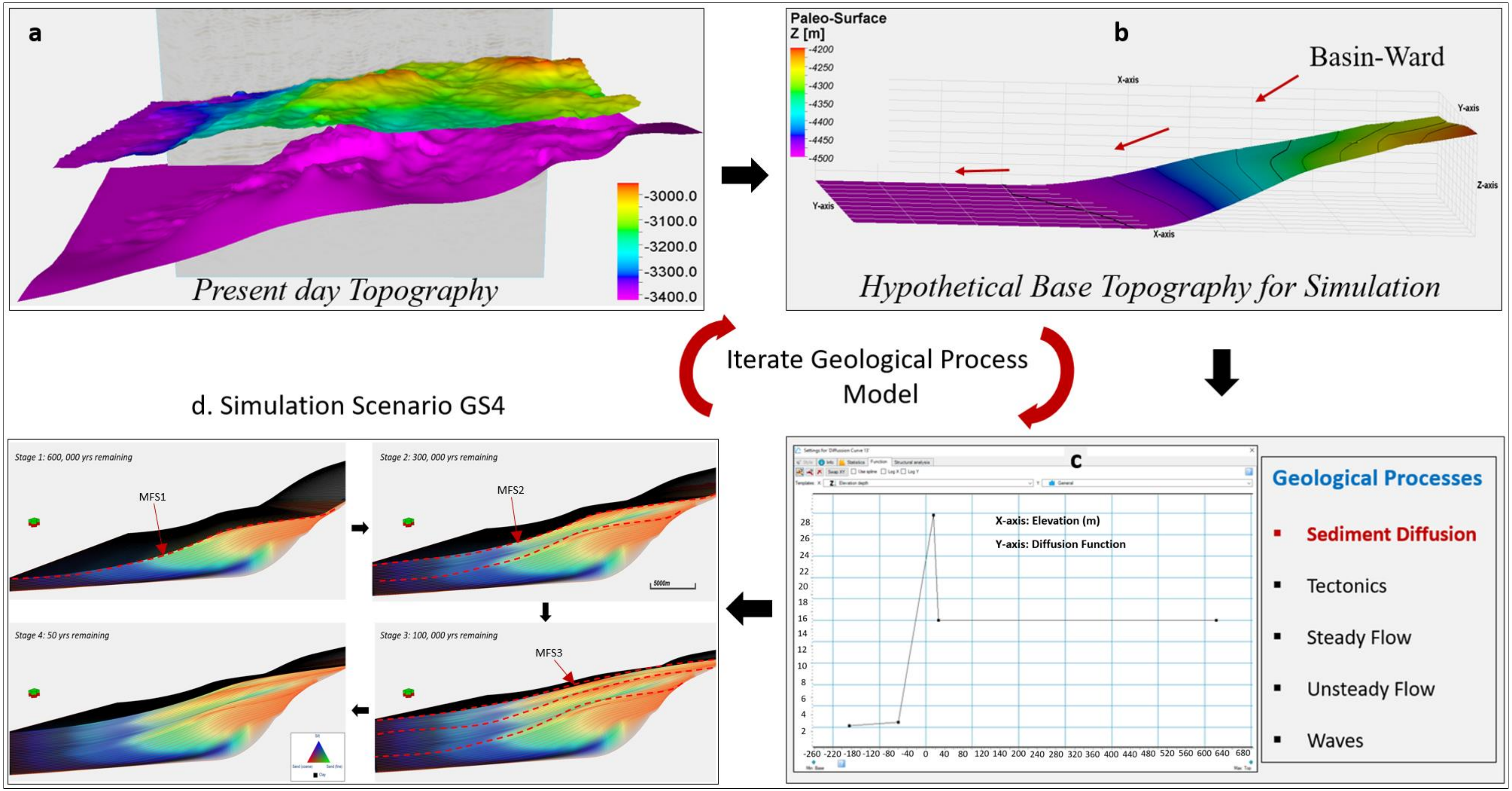

Fig 5. a. present-~~-~~day top and bottom topographic surfaces of the Hugin formation; b. hypothetical topographic surface ~~*derived*~~ from seismic data; c. geological processes involved in the forward stratigraphic simulation; d. forward stratigraphic models at different simulation time~~.~~ intervals.

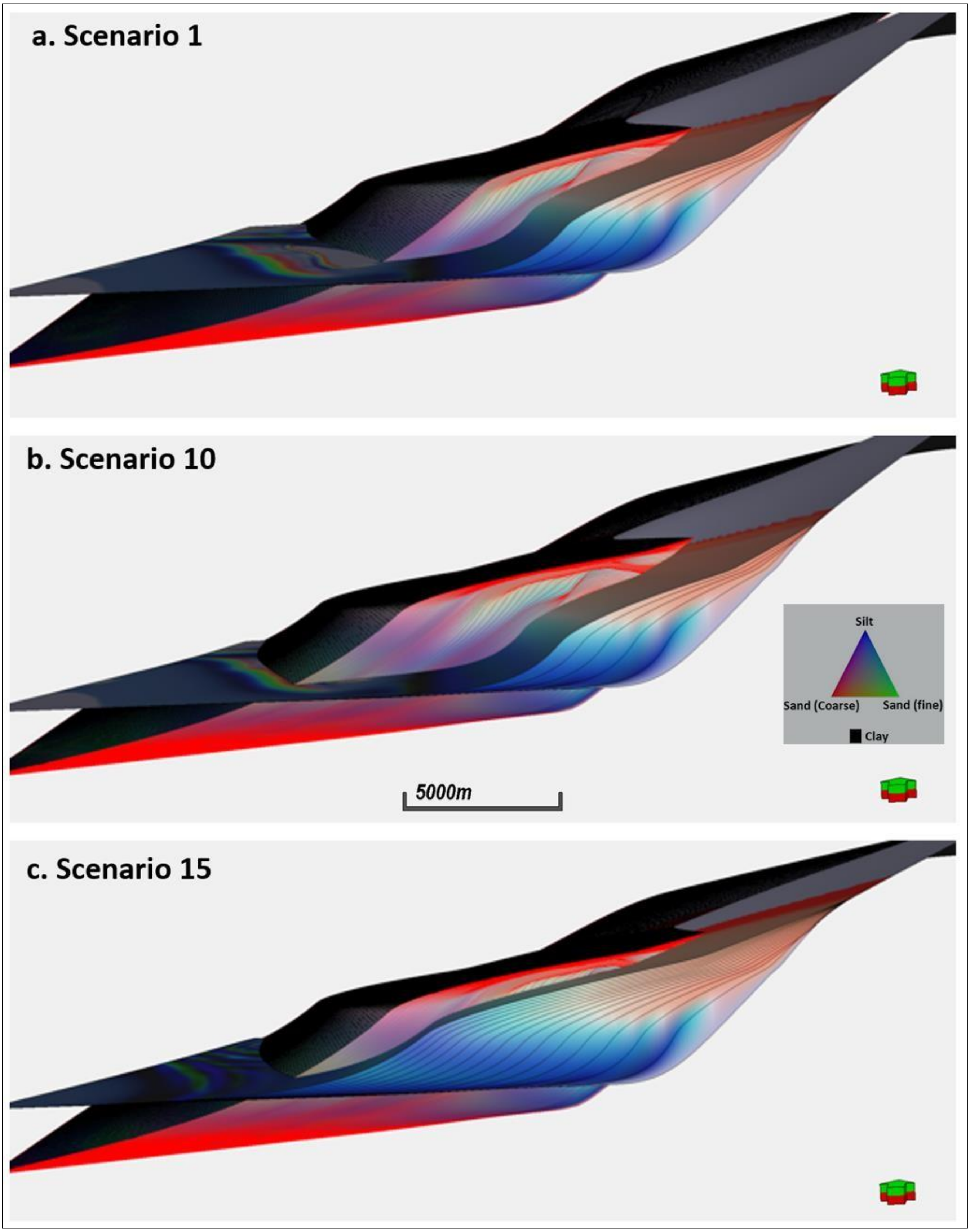
a. Scenario 1
b. Scenario 10
Silt
Sand (Coarse)
Sand (fine)
Clay
5000m
c. Scenario 15

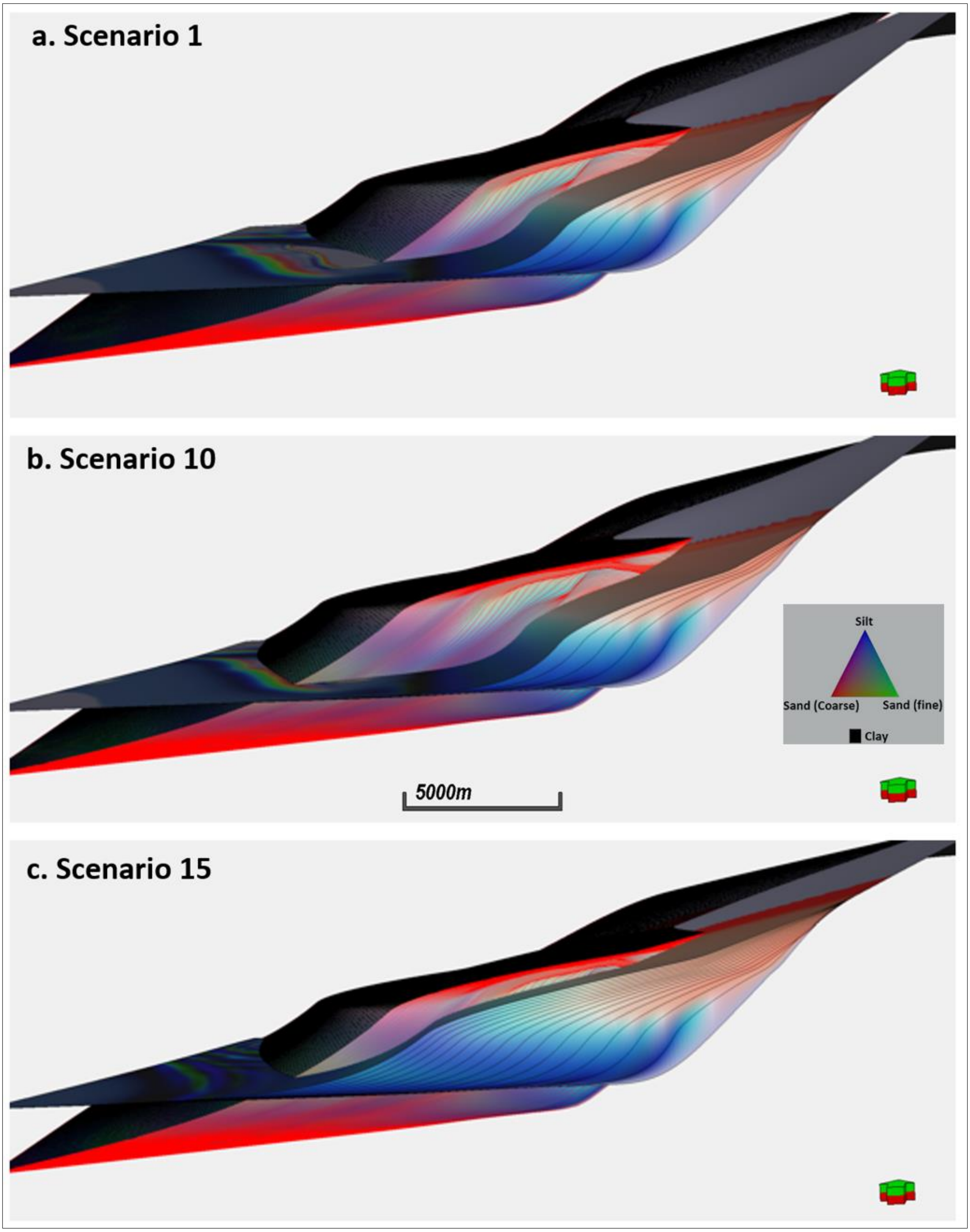

Fig 6. Stratigraphic simulation scenarios depicting sediment deposition in a shallow marine framework. **a.** scenario 1 involves equal proportions of sediment input, a relatively low subsidence rate and low water depth, **b.** scenario 10 uses high proportions of fine sand and silt (~~i.e.~~ 70%) in the sediment mix, abrupt changes in subsidence rate, and a relatively high water depth, c. scenario 15 involves very high proportions of fine sand and silt (~~i.e.~~ 80%), steady rate of subsidence and uplift in the sediment source area, and a relatively low water depth.

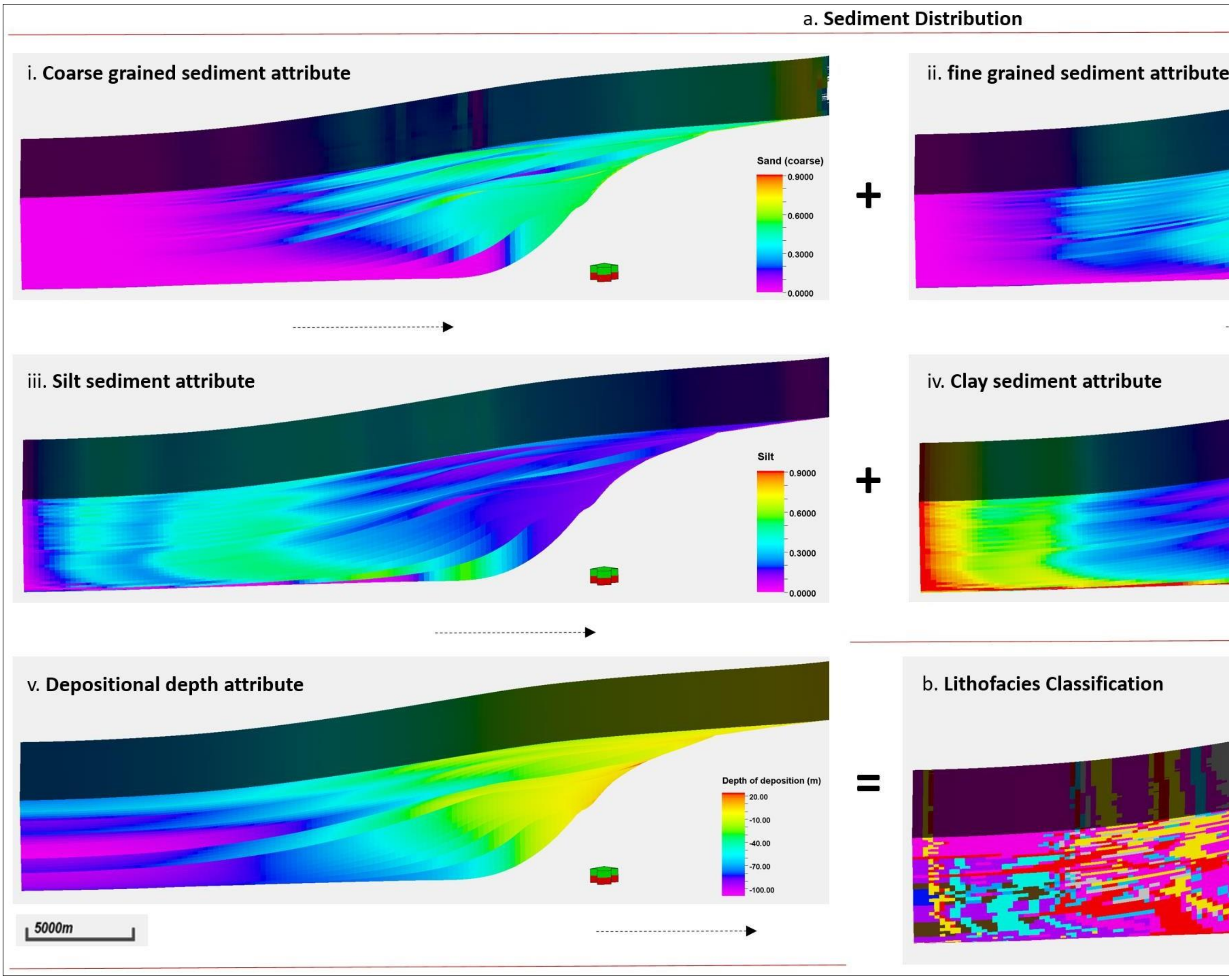

a. Sediment Distribution
i. Coarse grained sediment attribute
Sand (coarse)
0.9000
0.6000
0.3000
0.0000
ii. fine grained sediment attribute
iii. Silt sediment attribute
Silt
0.9000
0.6000
0.3000
0.0000
iv. Clay sediment attribute
v. Depositional depth attribute
Depth of deposition (m)
20.00
-10.00
-40.00
-70.00
-100.00
5000m
b. Lithofacies Classification

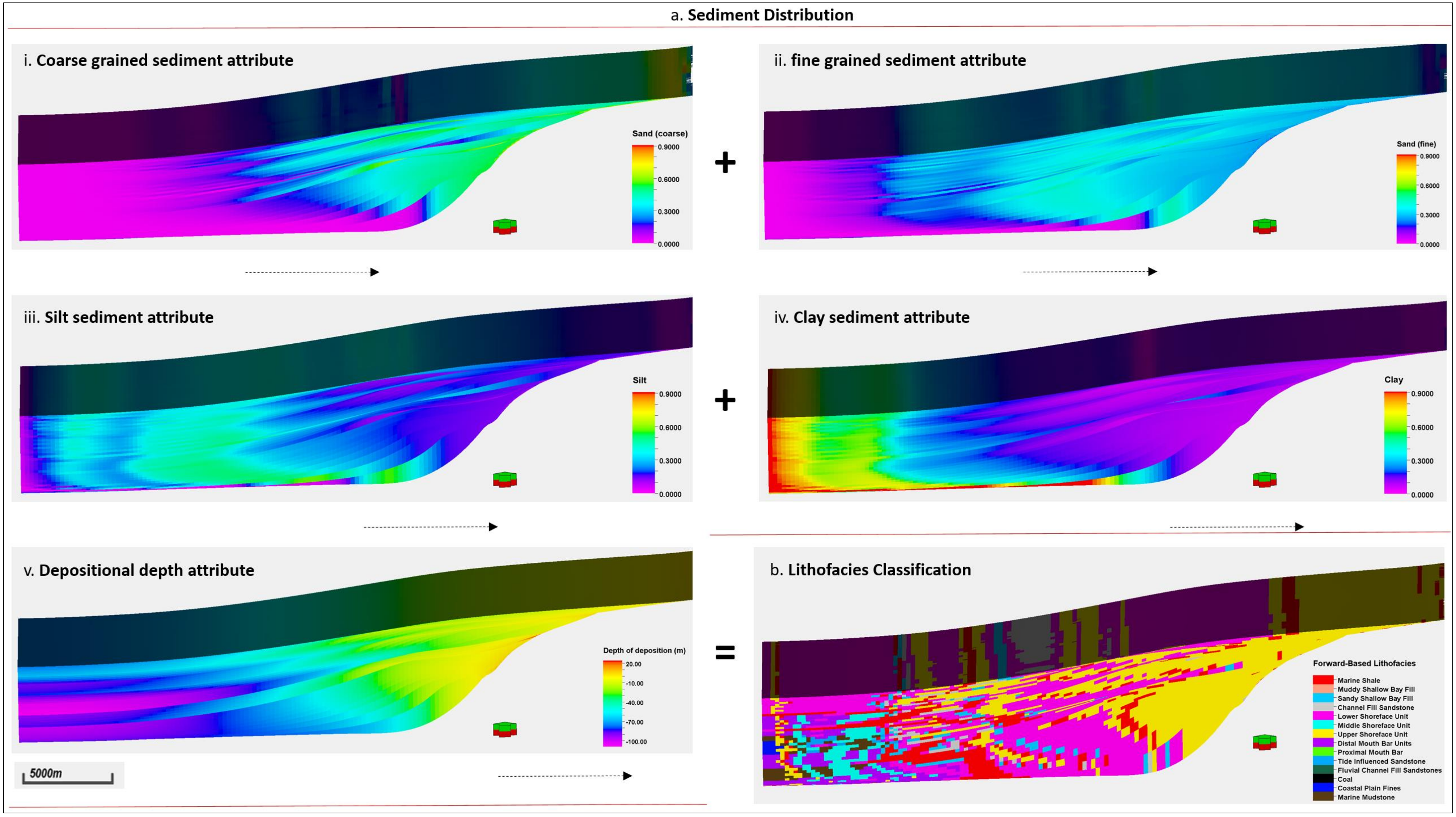

Fig 7 a. Sediment distribution patterns in the geological process modeling software. b. lithofacies classification using the property calculator tool in Petrel™.

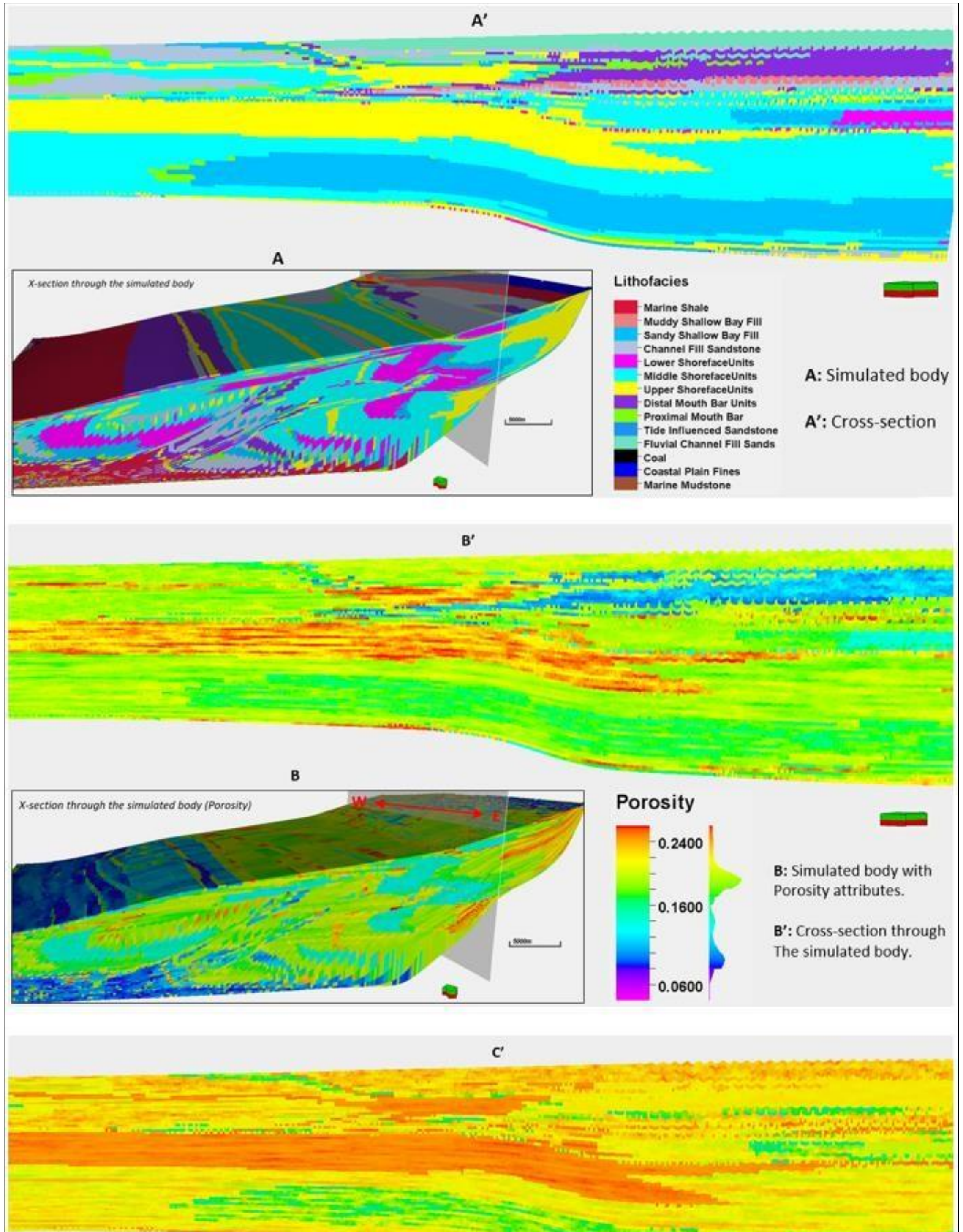

A'
A
X-section through the simulated body
Lithofacies
Marine Shale
Muddy Shallow Bay Fill
Sandy Shallow Bay Fill
Channel Fill Sandstone
Lower ShorefaceUnits
Middle ShorefaceUnits
Upper ShorefaceUnits
Distal Mouth Bar Units
Proximal Mouth Bar
Tide Influenced Sandstone
Fluvial Channel Fill Sands
Coal
Coastal Plain Fines
Marine Mudstone
A: Simulated body
A': Cross-section
B'
B
X-section through the simulated body (Porosity)
W
E
Porosity
0.2400
0.1600
0.0600
B: Simulated body with
Porosity attributes.
B': Cross-section through
The simulated body.
C'

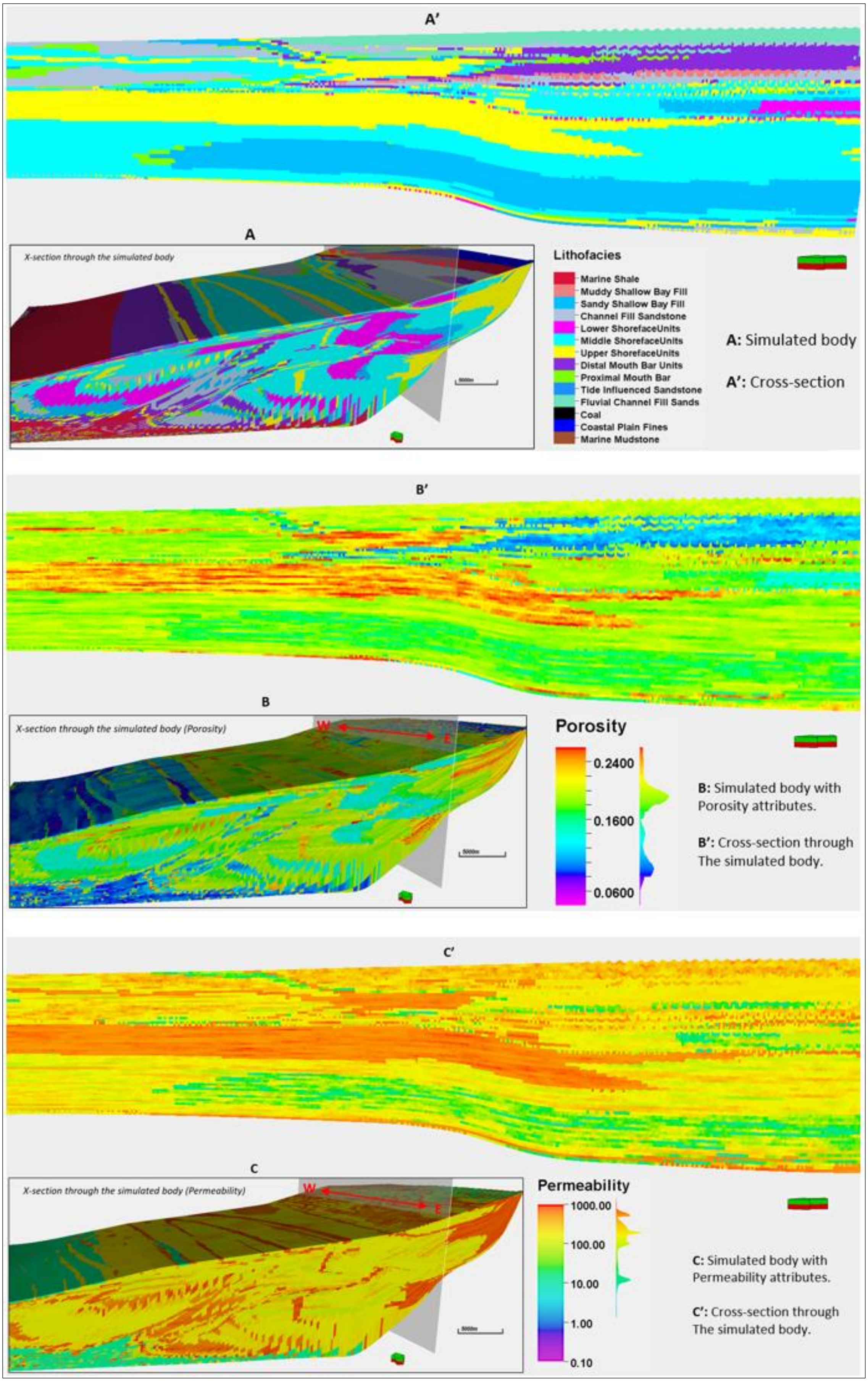
A'
A
X-section through the simulated body
Lithofacies
Marine Shale
Muddy Shallow Bay Fill
Sandy Shallow Bay Fill
Channel Fill Sandstone
Lower ShorefaceUnits
Middle ShorefaceUnits
Upper ShorefaceUnits
Distal Mouth Bar Units
Proximal Mouth Bar
Tide Influenced Sandstone
Fluvial Channel Fill Sands
Coal
Coastal Plain Fines
Marine Mudstone
A: Simulated body
A': Cross-section
B'
B
X-section through the simulated body (Porosity)
W
E
Porosity
0.2400
0.1600
0.0600
B: Simulated body with Porosity attributes.
B': Cross-section through The simulated body.
C'
C
X-section through the simulated body (Permeability)
W
E
Permeability
1000.00
100.00
10.00
1.00
0.10
C: Simulated body with Permeability attributes.
C': Cross-section through The simulated body.

Fig 8. ~~*Property*~~ Lithofacies, porosity and permeability characterization in the stratigraphic ~~*using*~~model through the property calculator tool in ~~*Petrel*~~Petrel™. Also ~~*showing*~~, is a cross-sectional view ~~*through*~~of the ~~*model.*~~3-D models.

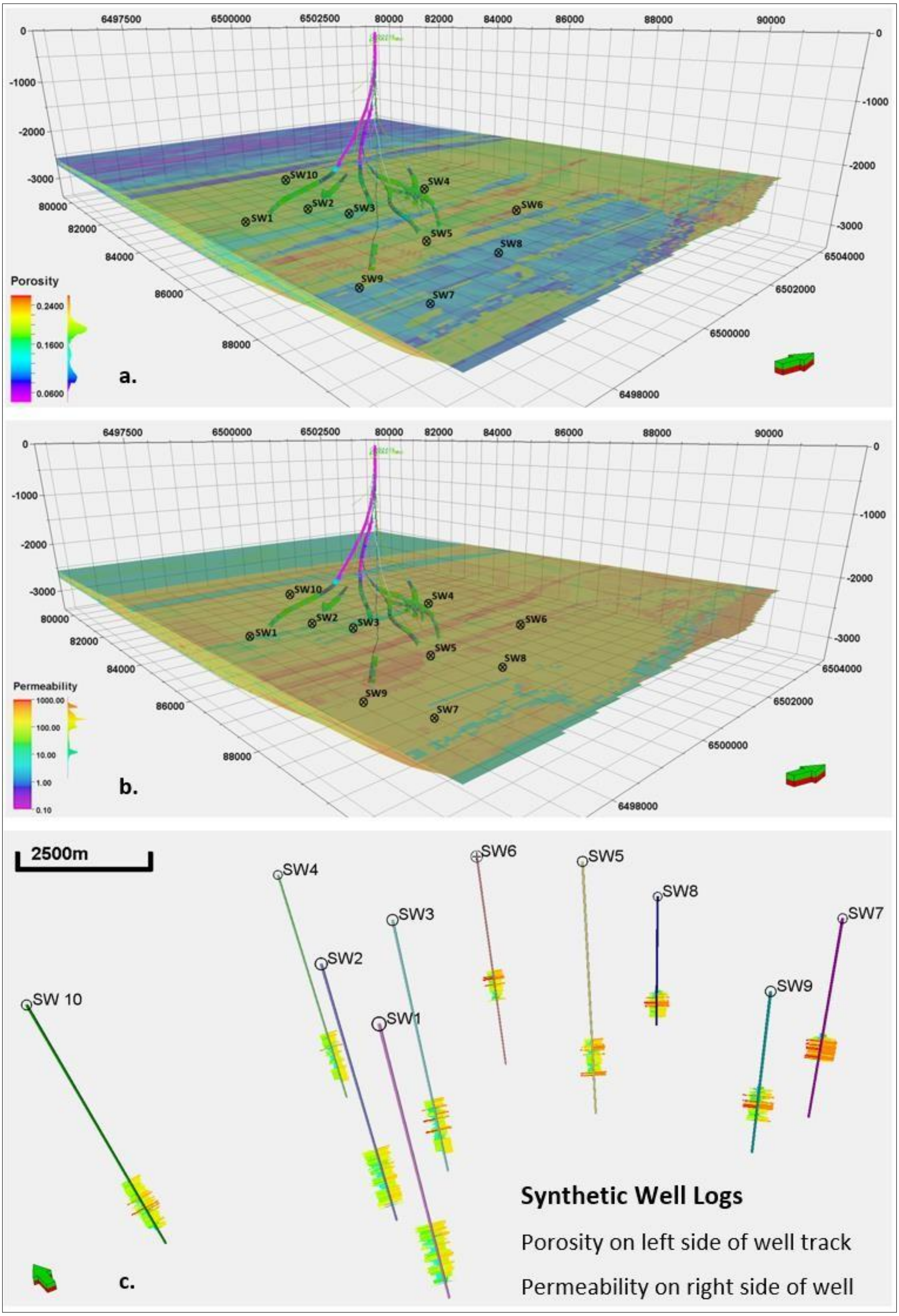

Porosity
a.
Permeability
b.
2500m
SW 10
SW1
SW2
SW3
SW4
SW5
SW6
SW7
SW8
SW9
Synthetic Well Logs
Porosity on left side of well track
Permeability on right side of well
c.

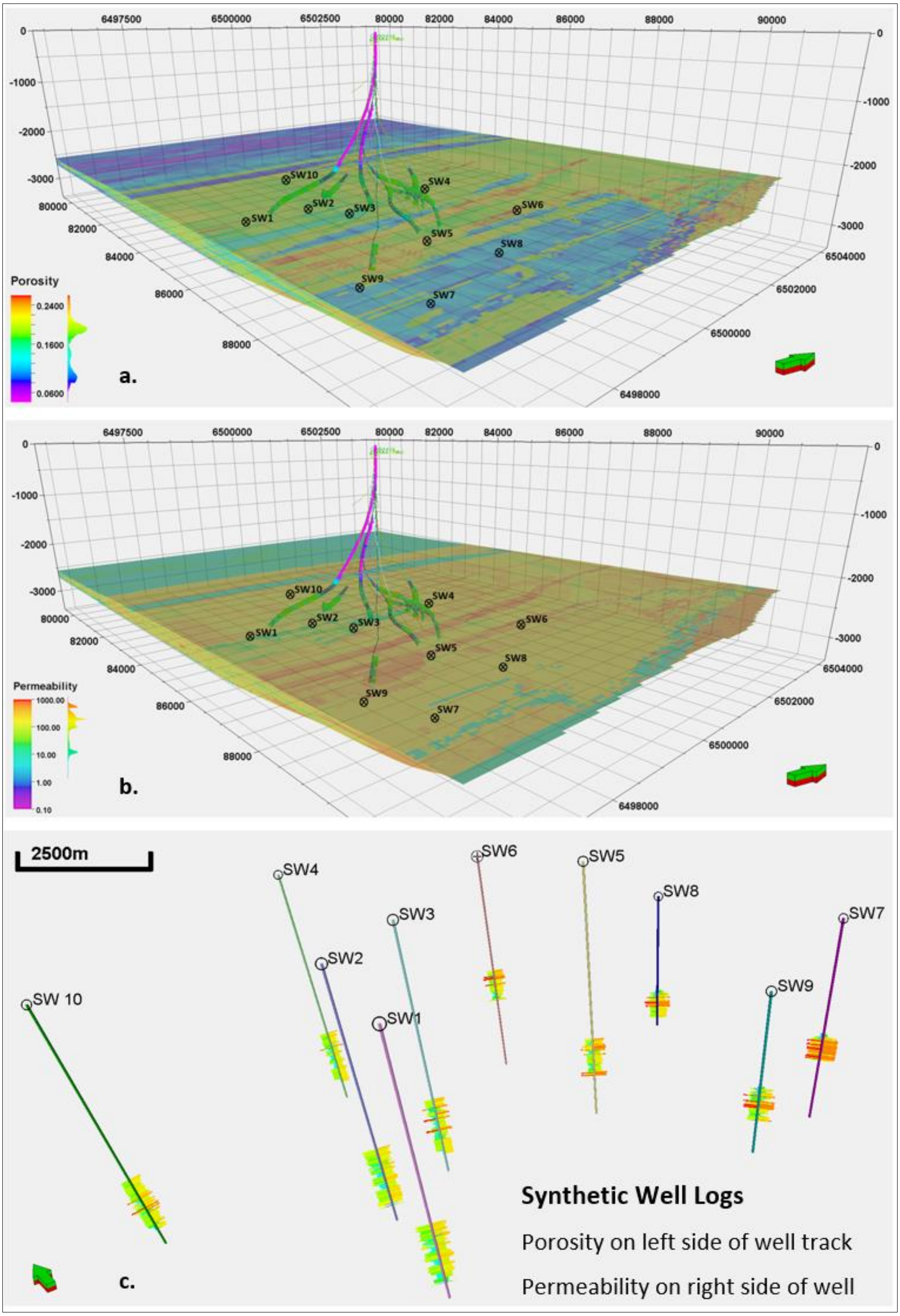

Fig 9. Synthetic wells ~~derived~~ from a forward stratigraphic-driven porosity and permeability ~~models.~~model. The average separation distance between the synthetic wells shown in Figure 9c is about 0.9 km apart (maximum and minimum separation distance of 1.3 km and 0.65 km, respectively).

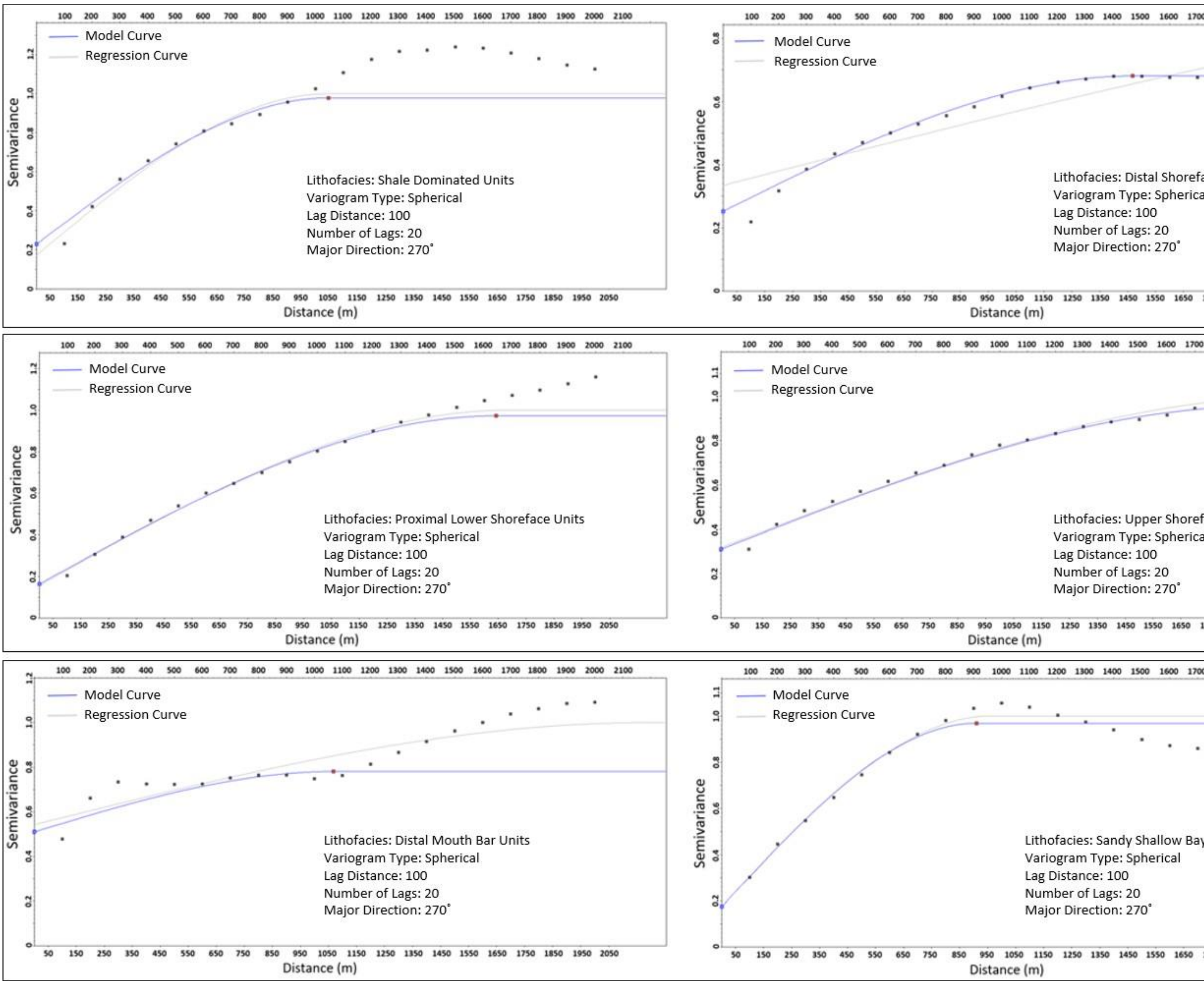
Model Curve
Regression Curve
Semivariance
Distance (m)
Lithofacies: Shale Dominated Units
Variogram Type: Spherical
Lag Distance: 100
Number of Lags: 20
Major Direction: 270˚
Lithofacies: Distal Shorefa
Variogram Type: Spherica
Lag Distance: 100
Number of Lags: 20
Major Direction: 270˚
Lithofacies: Proximal Lower Shoreface Units
Variogram Type: Spherical
Lag Distance: 100
Number of Lags: 20
Major Direction: 270˚
Lithofacies: Upper Shoref
Variogram Type: Spherica
Lag Distance: 100
Number of Lags: 20
Major Direction: 270˚
Lithofacies: Distal Mouth Bar Units
Variogram Type: Spherical
Lag Distance: 100
Number of Lags: 20
Major Direction: 270˚
Lithofacies: Sandy Shallow Bay
Variogram Type: Spherical
Lag Distance: 100
Number of Lags: 20
Major Direction: 270˚

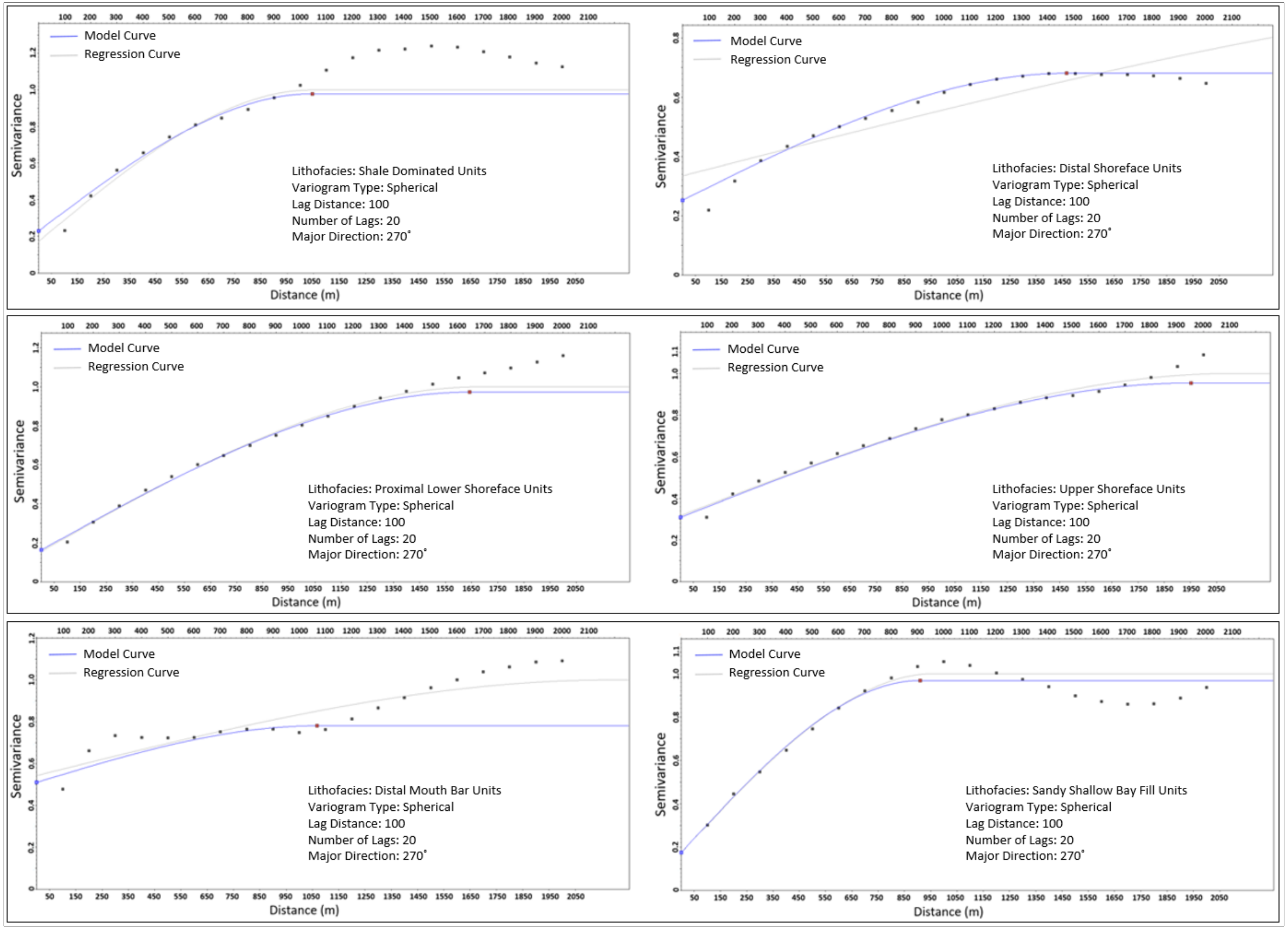
Model Curve
Regression Curve
Lithofacies: Shale Dominated Units
Variogram Type: Spherical
Lag Distance: 100
Number of Lags: 20
Major Direction: 270˚
Semivariance
Distance (m)
Model Curve
Regression Curve
Lithofacies: Distal Shoreface Units
Variogram Type: Spherical
Lag Distance: 100
Number of Lags: 20
Major Direction: 270˚
Semivariance
Distance (m)
Model Curve
Regression Curve
Lithofacies: Proximal Lower Shoreface Units
Variogram Type: Spherical
Lag Distance: 100
Number of Lags: 20
Major Direction: 270˚
Semivariance
Distance (m)
Model Curve
Regression Curve
Lithofacies: Upper Shoreface Units
Variogram Type: Spherical
Lag Distance: 100
Number of Lags: 20
Major Direction: 270˚
Semivariance
Distance (m)
Model Curve
Regression Curve
Lithofacies: Distal Mouth Bar Units
Variogram Type: Spherical
Lag Distance: 100
Number of Lags: 20
Major Direction: 270˚
Semivariance
Distance (m)
Model Curve
Regression Curve
Lithofacies: Sandy Shallow Bay Fill Units
Variogram Type: Spherical
Lag Distance: 100
Number of Lags: 20
Major Direction: 270˚
Semivariance
Distance (m)

Fig 10. Variogram model of dominant lithofacies units ~~extracted~~ from the ~~FSM~~forward stratigraphic model. The points indicate the number of lags in the variogram. The distance between these lags is about 100 m. This figure shows the lags between sample pairs for calculating the variogram in the major direction (NE-SW) of the stratigraphic model.

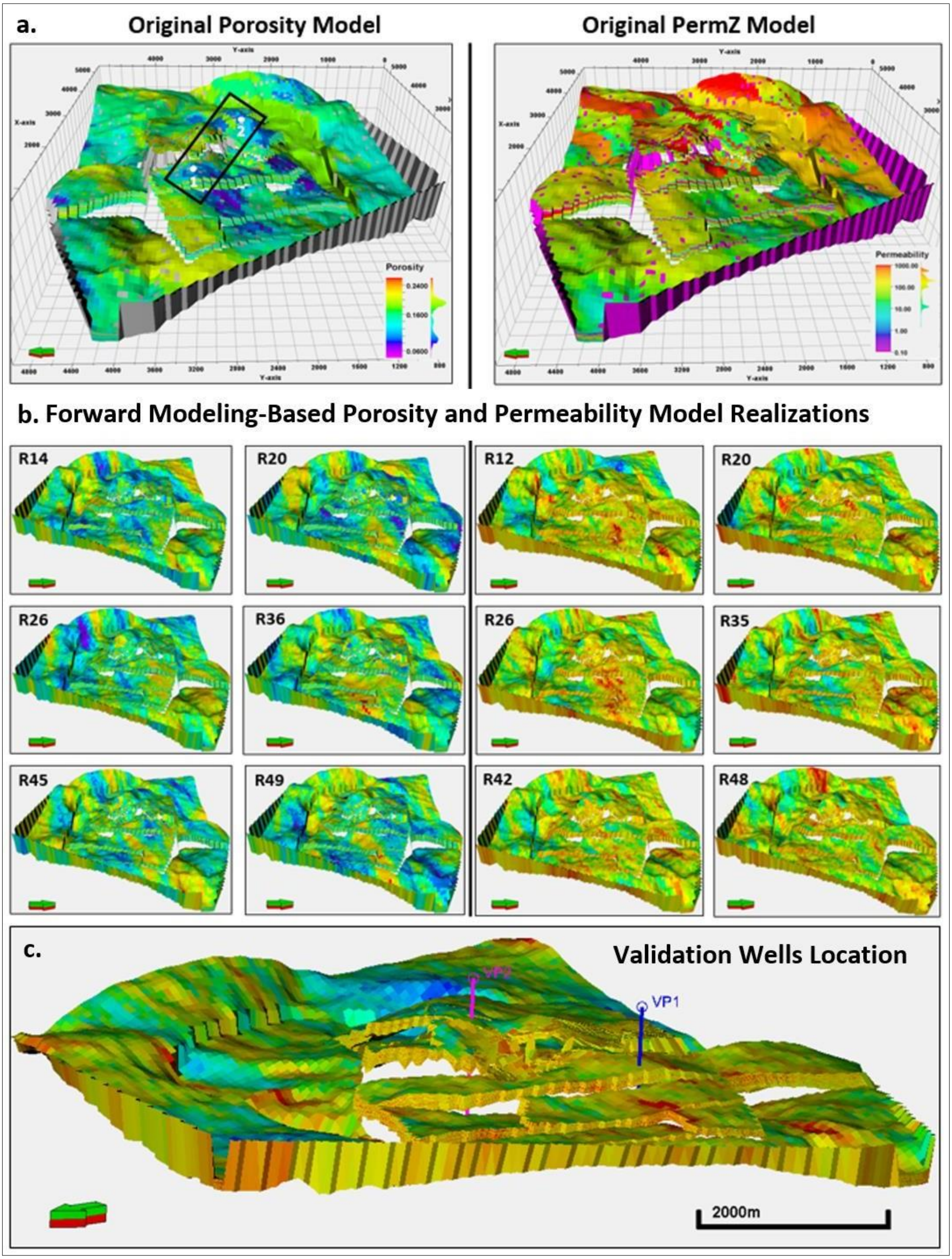

a.
Original Porosity Model
Original PermZ Model
Porosity
Permeability
b. Forward Modeling-Based Porosity and Permeability Model Realizations
R14
R20
R12
R20
R26
R36
R26
R35
R45
R49
R42
R48
c.
Validation Wells Location
VP1
2000m

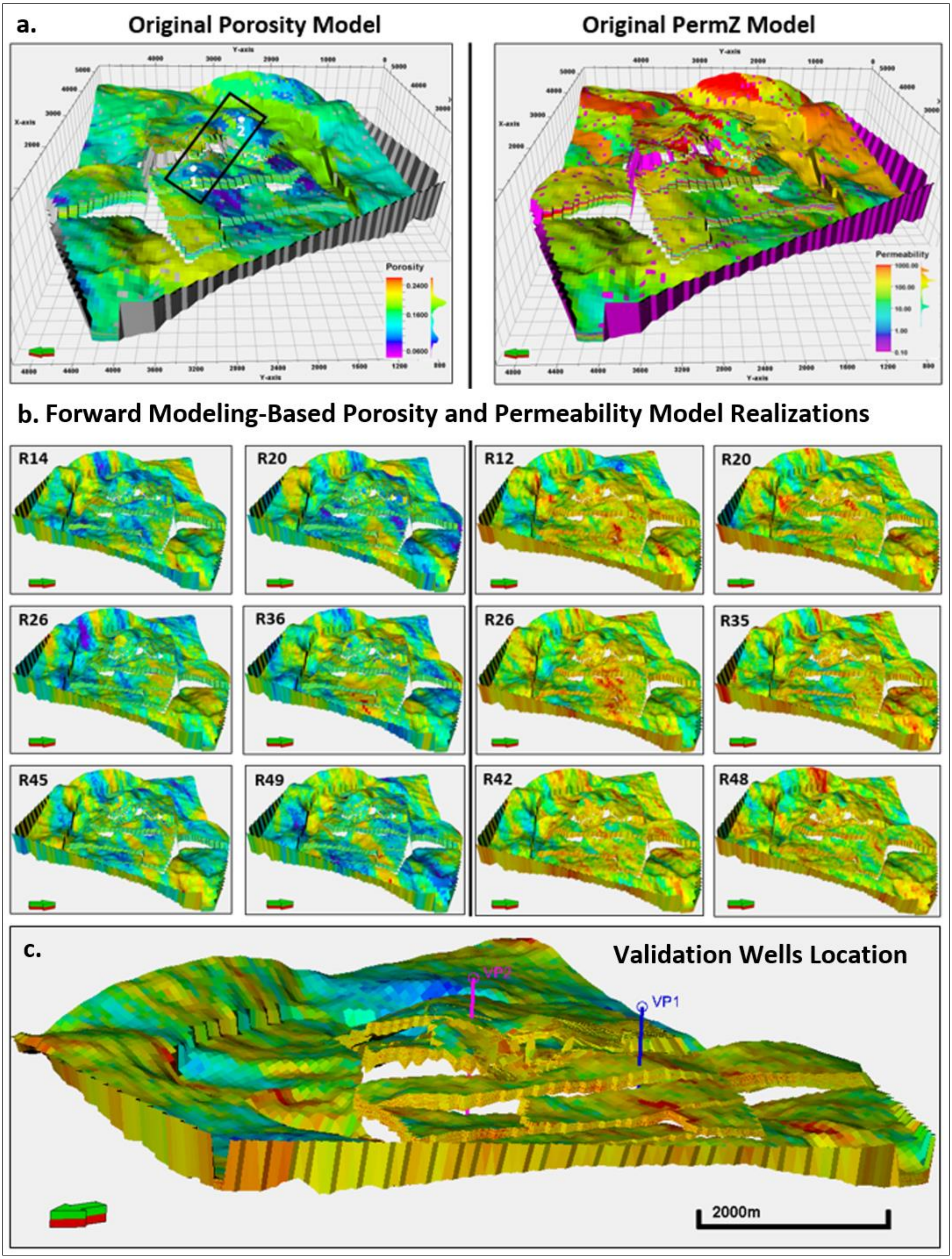

Fig 11. ~~Comparing original~~Original Volve field model ~~to~~vs the forward modeling-based models. Realizations 16, 20, 26, 36, 45, and 49 on the left half are porosity models, ~~whilst~~whiles realizations 12, 20, 26, 35, 42, and 48 on the right half ~~show~~are permeability models.

a. Validation Well 1

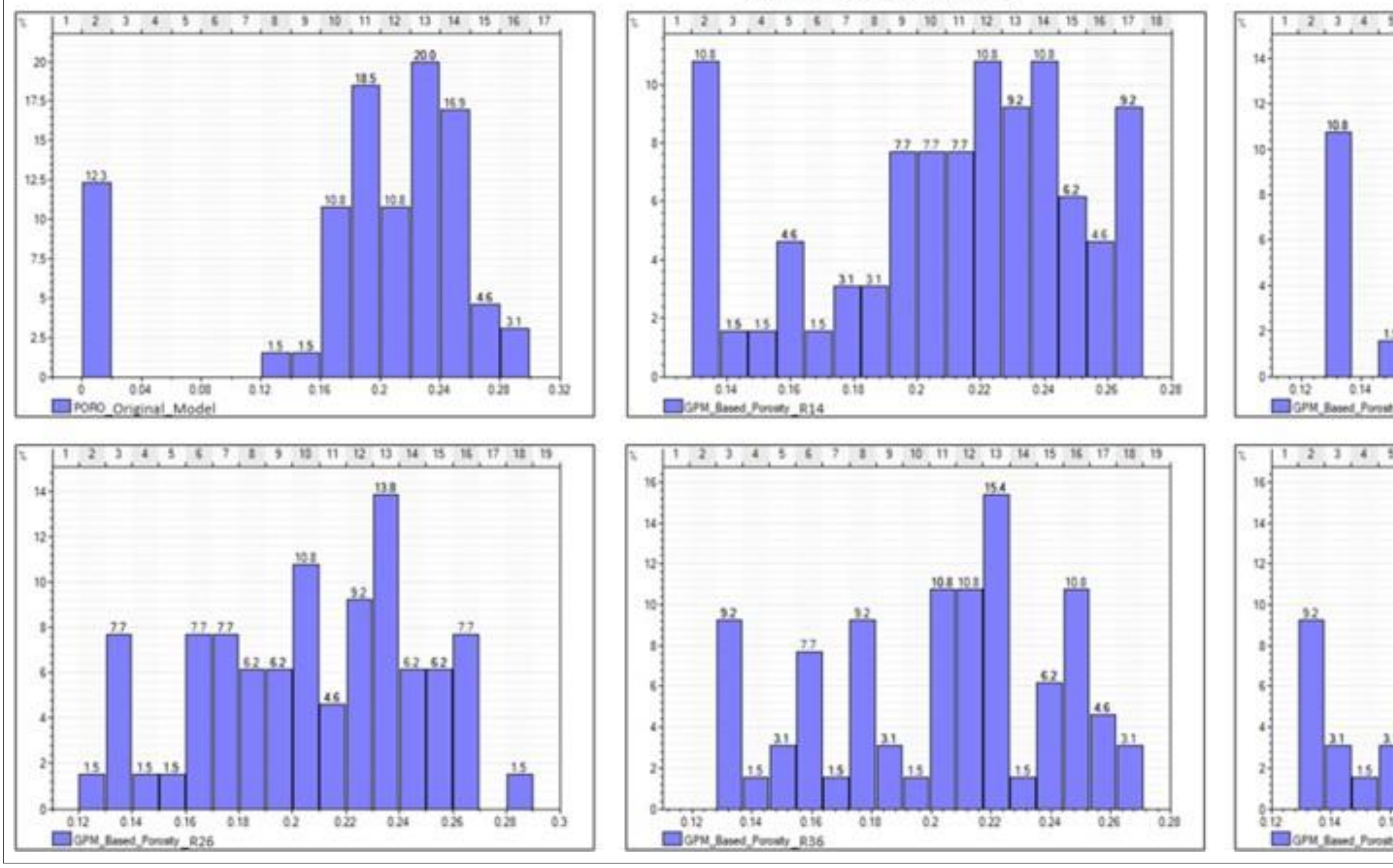

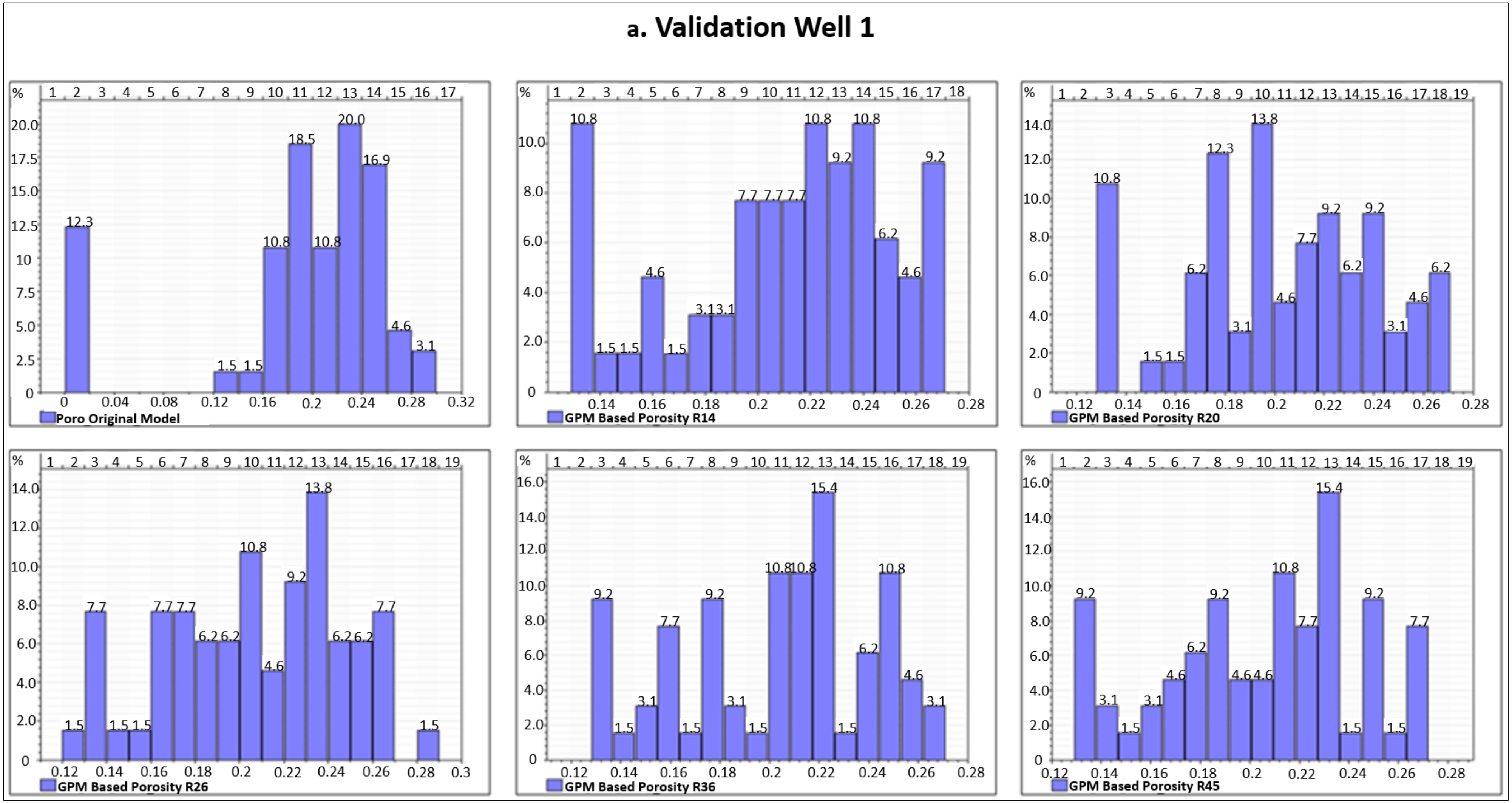

Figure 12a. ~~Samples of~~ Comparing porosity in validation Well 1 in five selected realizations , and ~~how it compares to~~ the ~~samples~~original model at similar vertical ~~interval in the original porosity and permeability models.~~

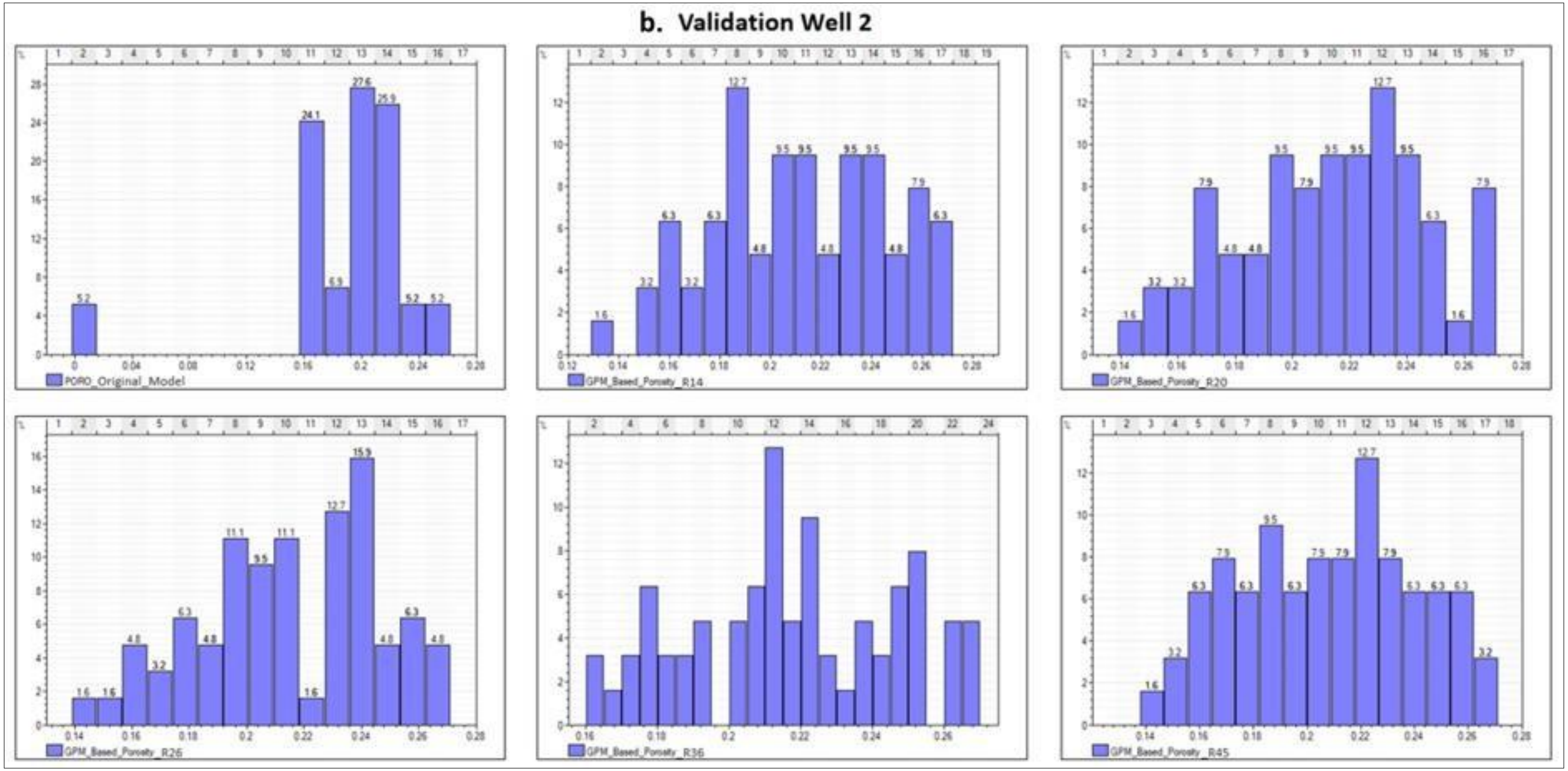
b. Validation Well 2
PORO_Original_Model
GPM_Based_Porosity_R14
GPM_Based_Porosity_R20
GPM_Based_Porosity_R26
GPM_Based_Porosity_R36
GPM_Based_Porosity_R45

intervals.

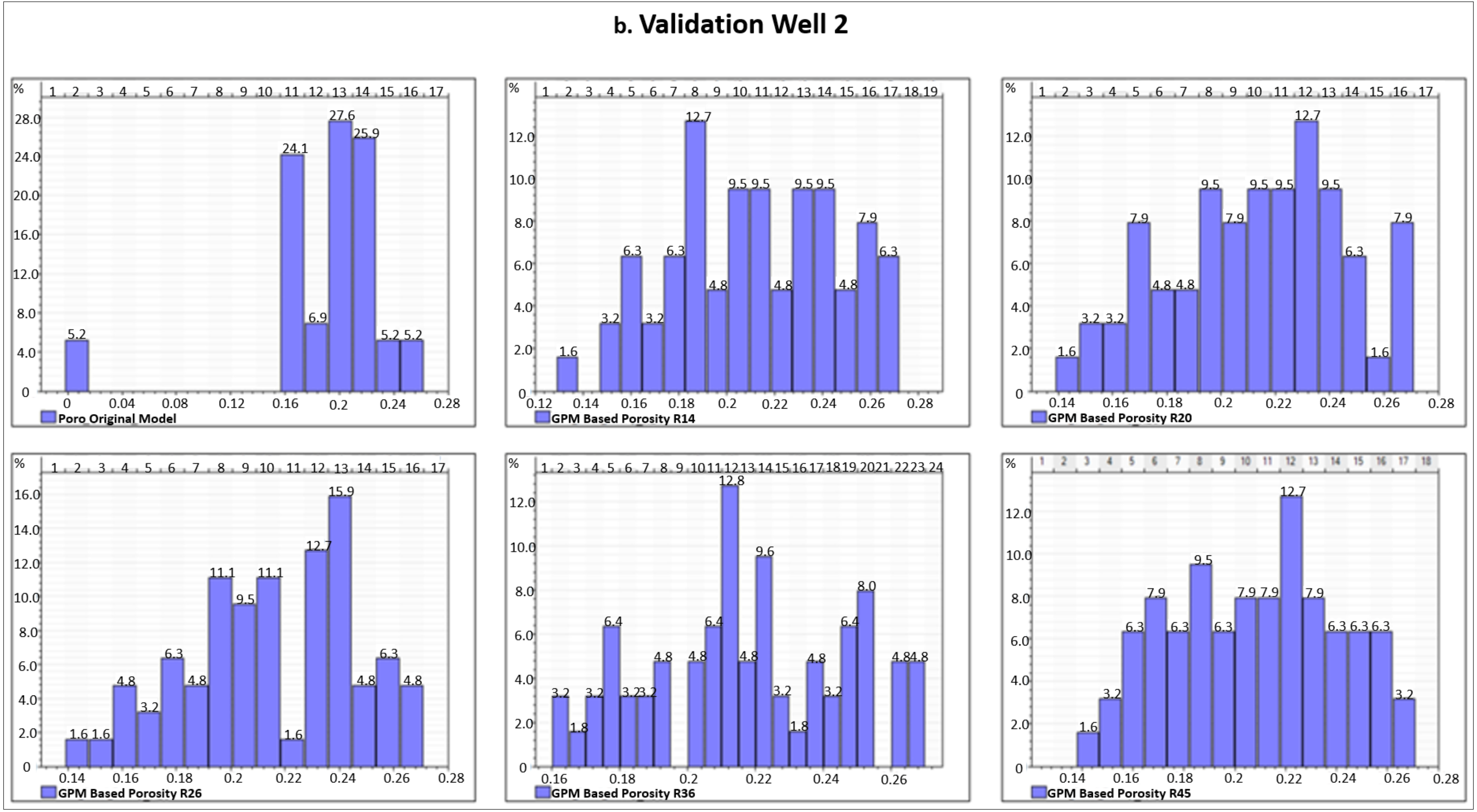

Figure 12b. ~~Samples of~~ Comparing porosity in validation Well 2 ~~in~~ five selected realizations , and ~~how it compares to~~ the ~~samples~~original model at similar vertical ~~interval in the original porosity and permeability models.~~

intervals.

Code	Facies	Description	Thickness (t); extent (l)	Wireline-log Attribute	Interpretation
A	A1	Parallel-laminated mudstone with occasional siltstone inputs. Monospecific pattern of disorder bivalves parallel to bedding.	t= 30-425 cm l= 6 to 29 km	GR= 41-308 API DT= 225-355 μsm^{-1} NPHI= 0.17-0.45 v/v RHOB= 2280-2820 gcm^{-3}	Restricted marine shale
	A2	Interbedded claystone and very fine-grained sandstone; non-parallel and wavy lamination. Scarcely bivalve shells oriented parallel to bedding.	t= 10-725 cm l = 8 km to 13 km	GR= 71-65 API DT= 189-268 μsm^{-1} NPHI=? RHOB= 2280-2820 gcm^{-3}	Muddy Shallow bay-fill
	A3	Fine to medium grained sandstone; moderately to well sorted grains. Wavy bedding, cross bedding, rare wave ripples	t= 60-370 cm l <8 km	GR= 18-46 API DT= 199-314 μsm^{-1} NPHI= 0.07-0.52 v/v RHOB= 1690-2745 gcm^{-3}	Sandy shallow bay-fill
	A4	Coarse to fine-grained sandstones with alternating upward fining to coarsening trend. Moderately sorted grains. Sparse sedimentary structures.	t= 250-500 cm l = 1.8 km to 4.2 km	GR= 7-35 API DT= 175-230 μsm^{-1} NPHI= 0.038-0.146 v/v RHOB= 2280-2820 gcm^{-3}	Marine channel-fill sandstones
B	B1	Upward-coarsening siltstone to fine-grained moderate sorted sandstones, with shell debris, and quartz granules.	t= 30-480 cm l = <2 km	GR= 18-80 API DT= 168-291 μsm^{-1} NPHI= 0.038-0.191 v/v RHOB= 2322-2723 gcm^{-3}	Distal lower shoreface
	B2	Very fine-fine grained, moderate to well sorted sandstone. Fine grained carbonaceous laminae, typically low angle cross beds.	t= 130-440 cm l = 1.7 km – 8 km	GR= 20-56 API DT= 179-277 μsm^{-1} NPHI= 0.048-0.168 v/v RHOB= 2314-2696 gcm^{-3}	Proximal lower shoreface
	B3	Coarsening upward, cross laminated, fine to medium grained, well sorted sandstone; consist carbonaceous fragments	t= 425-800 cm l = 1.7 km – 8 km	GR= 15-25 API DT= 250-275 μsm^{-1} NPHI= 0.09-0.113 v/v RHOB= 2271-2342 gcm^{-3}	Upper Shoreface
C	C1	Highly bioturbated siltstone to very fine sandstones, which has beds of rounded granules	t= 175-1010 cm l = 7.2 km – 19.6 km	GR= 20-80 API DT= 230-260 μsm^{-1} NPHI= 0.08-0.169 v/v RHOB= 2327-2521 gcm^{-3}	Distal mouth bar
	C2	Very fine to fine grained sandstones; low angle cross-bedding.	t= 290-775 cm l = < 5 km	GR= 12-58 API DT= 167-397 μsm^{-1} NPHI= 0.05-0.595 v/v RHOB= 1612-2705 gcm^{-3}	Proximal mouth bar

Table 1 Lithofacies-associations in the Hugin formation, Volve Field (after Kieft et al. 2011).

Code	Facies	Description	Thickness (t); Extent (l)	Wireline-log Attribute	Interpretation
A	A1	Parallel-laminated mudstone with occasional siltstone inputs. Monospecific pattern of disorder bivalves parallel to bedding.	t = 30 - 425 cm l = 6 - 29 km	GR = 41 - 308 API DT = 225 - 355 μsm^{-1} NPHI = 0.17 - 0.45 v/v RHOB = 2280 - 2820 gcm^{-1}	Restricted marine shale
	A2	Inter-bedded claystone and very fine-grained sandstone; non-parallel and wavy lamination. Scarecely bivalve shells oriented parallel to bedding.	t = 10 - 725 cm l = 8 - 13 km	GR = 17 - 65 API DT = 189 - 268 μsm^{-1} NPHI =? RHOB = 2280 - 2820 gcm-1	Muddy hallow bay fill
	A3	Fine to medium grained sandstone; moderately to well sorted grain. Wavy bedding, cross bedding, rare wave ripples.	t = 60 - 370 cm l = 1 - 8 km	GR = 18 - 46 API DT = 199 - 268 μsm^{-1} NPHI = 0.07 - 0.52 v/v RHOB = 1690 - 2745 gcm-1	Sandy shallow bay fill
	A4	Parallel-laminated mudstone with occasional siltstone inputs. Monospecific pattern of disorder bivalves parallel to bedding.	t = 30 - 425 cm l = 6 - 29 km	GR = 7 - 35 API DT = 175 - 230 μsm^{-1} NPHI = 0.04 - 0.15 v/v RHOB = 2280 - 2820 gcm-1	Marine channel fill sandstone
B	B1	Upward coarsening siltstone to fine-grained; moderatley sorted sandstone. Shell debris and quartz granules.	t = 30 - 480 cm l = 1 - 2 km	GR = 18 - 80 API DT = 168 - 291 μsm^{-1} NPHI = 0.04 - 0.191 v/v RHOB = 2322 - 2723 gcm-1	Distal lower shoreface
	B2	Very fine-fine grained sandstone. Moderate to well sorted; fine grained carbonaceous laminae, typically low angle cross beds.	t = 130 - 440 cm l = 1.7 - 12 km	GR = 20 - 56 API DT = 179 - 277 μsm^{-1} NPHI = 0.05 - 0.168 v/v RHOB = 2314 - 2696 gcm-1	Proximal lower shoreface
	B3	Coaesening upward, cross laminated, fine to medium grainned sandstone; consist of carbonaceous fragments.	t = 425 - 800 cm l = 1.7 - 8 km	GR = 15 - 25 API DT = 250 - 275 μsm^{-1} NPHI = 0.09 - 0.113 v/v RHOB = 2271 - 2342 gcm-1	Upper shoreface
C	C1	Highly bioturbated siltstone to very fine sandstone, with beds of rounded granules.	t = 175 - 1010 cm l = 7.2 - 19.6 km	GR = 20 - 80 API DT = 230 - 260 μsm^{-1} NPHI = 0.08 - 0.169 v/v RHOB = 2327 - 2521 gcm-1	Distal mouth bar
	C2	Very fine to fine grained sandstone, low angle cross bedding.	t = 290 - 775 cm l = 1 - 5 km	GR = 12 - 58 API DT = 167 - 397 μsm^{-1} NPHI = 0.05 - 0.595 v/v RHOB = 1612 - 2705 gcm-1	Proximal mouth bar
D	D1	Fining upward coarse to fine grained sandstone. Stacked fining upward beds with rare coarse grained stringers.	t = 740 - 820 cm l = 1 - 2 km	GR = 8 - 134 API DT = 235 - 335 μsm^{-1} NPHI = 0.14 - 0.46 v/v RHOB = 2284 - 2570 gcm-1	Tidal influenced fluvial channel fill sandstone
	D2	Fining upward coarse to medium grained sandstone. Carbonaceous laminae and fragments. Sharp and cohessive contact at base of bed.	t = 580 cm l = < 2 km	GR = 9 - 34 API DT = 241 - 297 μsm^{-1} NPHI = 0.14 - 0.289 v/v RHOB = 2168 - 2447 gcm-1	fluvial channel fill sandstone
E	E1	Coal and carbonaceous shale. Basal contact typically parallel, although maybe undulose.	t = 30 - 520 cm l = 6 - 19.6 km	GR = 8 - 56 API DT = 313 - 427 μsm^{-1} NPHI = 0.24 - 0.529 v/v RHOB = 1930 - 2225 gcm-1	Coal
	E2	Alternating dark grey mudstone/claystone and siltstone to very fine grained sandstone. Wavy to non-parallel lamination.	t = 60 cm l = < 2 km	GR = 32 - 60 API DT = 358 - 415 μsm^{-1} NPHI = 0.43 - 0.49 v/v RHOB = 1994 - 2148 gcm-1	Coastal plain fines
F	F	Mudstone with rare siltstone beds. Parallel lamination, soft sediment deformation developed locally on top of beds.	t = section tot completely penetrated l = 1.7 - 36.7 km	GR = 4 - 134 API DT = 187 - 450 μsm^{-1} NPHI = 0.114 - 0.618 v/v RHOB = 1730 - 2925 gcm-1	Open marine shale

Table 2. Input parameters ~~applied in running the~~ for forward stratigraphic simulations in GPM™

	Initial Conditions- GPM Input Parameters												
	Simulation Duration	Sediment Type Proportion (%)				Avg. Water Velocity	Avg. Sediment Velocity	Erodibility	Diffusion Coefficient	Avg. Sea Level	Turbidite Event Interval	Steady Flow Iteration	Sediment Movement
GPM Scenarios (GS)	(Ma– 0a) Years	Sand (Coarse)	Sand (Fine)	Silt	Clay	(m/a)	(m/a)			Interval (m)	(/years)	(/hrs)	Coefficient
S1	0.02 – 0	25	25	25	25	0.11	0.03	0.35	0.11	30	2500	10	0.001
S2	0.25 – 0	25	25	25	25	0.15	0.03	0.45	0.15	70	1000	15	0.012
S3	0.5 – 0	25	25	25	25	0.11	0.02	0.55	0.11	120	1000	20	0.012
S4	0.7 – 0.05	25	25	25	25	0.08	0.02	0.35	0.08	100	500	25	0.0011
S5	1.5 – 0	15	35	30	20	0.15	0.04	0.50	0.15	80	5000	20	0.001
S6	3.0 – 0	50	25	15	10	0.13	0.04	0.50	0.13	70	5000	30	0.0012
S7	3.5 – 0	50	25	15	10	0.11	0.04	0.50	0.11	70	10000	15	0.001
S8	4.0 – 0	50	25	15	10	0.13	0.04	0.50	0.13	90	5000	20	0.0015
S9	4.5 – 0	15	45	25	15	0.1	0.02	0.45	0.1	50	10000	30	0.0012
S10	5.0 – 0	15	45	25	15	0.12	0.02	0.45	0.12	55	10000	35	0.0013
S11	5.5 - 0	15	45	25	15	0.12	0.02	0.45	0.12	40	5000	40	0.0013
S12	6.0 – 0	15	45	25	15	0.1	0.02	0.45	0.1	60	10000	35	0.0011
S13	6.5 – 0	10	25	55	10	0.13	0.03	0.48	0.13	100	20000	50	0.0010
S14	7.0 – 0	10	25	55	10	0.16	0.03	0.48	0.16	40	20000	45	0.0011
S15	7.5 – 0	10	25	55	10	0.13	0.03	0.48	0.13	40	20000	40	0.0012
S16	8.0 – 0	10	25	55	10	0.15	0.03	0.48	0.15	30	10000	30	0.0010
S17	8.5 – 0	10	25	45	20	0.14	0.02	0.45	0.14	50	50000	50	0.0010
S18	9.0 – 0	30	30	18	22	0.13	0.02	0.52	0.13	60	25000	35	0.0012
S19	9.5 – 0	30	40	12	18	0.12	0.02	0.55	0.12	55	25000	20	0.0013
S20	10.0 - 0	30	42	18	10	0.11	0.01	0.40	0.11	50	5000	15	0.0011

Sediment Property								
Sediment Type	**Diameter**	**Density**	**Initial Porosity**	**Initial Permeability**	**Compacted Porosity**	**Compaction**	**Compacted Permeability**	**Erodibility**
Coarse Grained Sand	1.0 mm	2.70 g/cm³	0.21 m³/m³	500 mD	0.25 m³/m³	5000 KPa	50 mD	0.6
Fine Grained Sand	0.1 mm	2.70 g/cm³	0.3 m³/m³	100 mD	0.15 m³/m³	2500 KPa	5 mD	0.45
Silt	0.01 mm	2.65 g/cm³	0.38 m³/m³	50 mD	0.12 m³/m³	1200 KPa	2 mD	0.3
Clay	0.001 mm	2.65 g/cm³	0.48 m³/m³	5 mD	0.05 m³/m³	500 KPa	0.1 mD	0.15

Initial Conditions- GPM Input Parameters

GPM Scenarios (GS)	Simulation Duration (Ma– 0a) Years	Sediment Type Proportion (%) Sand (Coarse)	Sand (Fine)	Silt	Clay	Avg. Water Velocity (m/a)	Avg. Sediment Velocity (m/a)	Erodibility	Diffusion Coefficient	Avg. Sea Level Interval (m)	Turbidite Event Interval (/years)	Steady Flow Iteration (/hrs)	Sediment Movement Coefficient
S1	0.02 – 0	25	25	25	25	0.11	0.03	0.35	0.11	30	2500	10	0.001
S2	0.25 – 0	25	25	25	25	0.15	0.03	0.45	0.15	70	1000	15	0.012
S3	0.5 – 0	25	25	25	25	0.11	0.02	0.55	0.11	120	1000	20	0.012
S4	0.7 – 0.05	25	25	25	25	0.08	0.02	0.35	0.08	100	500	25	0.0011
S5	1.5 – 0	15	35	30	20	0.15	0.04	0.50	0.15	80	5000	20	0.001
S6	3.0 – 0	50	25	15	10	0.13	0.04	0.50	0.13	70	5000	30	0.0012
S7	3.5 – 0	50	25	15	10	0.11	0.04	0.50	0.11	70	10000	15	0.001
S8	4.0 – 0	50	25	15	10	0.13	0.04	0.50	0.13	90	5000	20	0.0015
S9	4.5 – 0	15	45	25	15	0.1	0.02	0.45	0.1	50	10000	30	0.0012
S10	5.0 – 0	15	45	25	15	0.12	0.02	0.45	0.12	55	10000	35	0.0013
S11	5.5 - 0	15	45	25	15	0.12	0.02	0.45	0.12	40	5000	40	0.0013
S12	6.0 – 0	15	45	25	15	0.1	0.02	0.45	0.1	60	10000	35	0.0011
S13	6.5 – 0	10	25	55	10	0.13	0.03	0.48	0.13	100	20000	50	0.0010
S14	7.0 – 0	10	25	55	10	0.16	0.03	0.48	0.16	40	20000	45	0.0011
S15	7.5 – 0	10	25	55	10	0.13	0.03	0.48	0.13	40	20000	40	0.0012
S16	8.0 – 0	10	25	55	10	0.15	0.03	0.48	0.15	30	10000	30	0.0010
S17	8.5 – 0	10	25	45	20	0.14	0.02	0.45	0.14	50	50000	50	0.0010
S18	9.0 – 0	30	30	18	22	0.13	0.02	0.52	0.13	60	25000	35	0.0012
S19	9.5 – 0	30	40	12	18	0.12	0.02	0.55	0.12	55	25000	20	0.0013
S20	10.0 - 0	30	42	18	10	0.11	0.01	0.40	0.11	50	5000	15	0.0011

Sediment Property

Sediment Type	Diameter	Density	Initial Porosity	Initial Permeability	Compacted Porosity	Compaction	Compacted Permeability	Erodibility
Coarse Grained Sand	1.0 mm	2.70 g/cm^3	0.21 m^3/m^3	500 mD	0.25 m^3/m^3	5000 KPa	50 mD	0.6
Fine Grained Sand	0.1 mm	2.70 g/cm^3	0.3 m^3/m^3	100 mD	0.15 m^3/m^3	2500 KPa	5 mD	0.45
Silt	0.01 mm	2.65 g/cm^3	0.38 m^3/m^3	50 mD	0.12 m^3/m^3	1200 KPa	2 mD	0.3
Clay	0.001 mm	2.65 g/cm^3	0.48 m^3/m^3	5 mD	0.05 m^3/m^3	500 KPa	0.1 mD	0.15

Table 3. Lithofacies classification in the forward stratigraphic model~~; showing the command used~~ in the property calculator tool in Petrel™.

Lithofacies Classification		
Facies Code	**Lithofacies**	**Command Used in Petrel's Property Calculator**
0	Marine Shale	If(Sand_fine>=0.19 And Sand_fine<=0.21 Or Silt>=0.19 And Silt<=0.2 Or Clay>=0.2 And Clay<=0.21 Or Depth_of_deposition>=-82 And Depth_of_deposition<=-78)
1	Muddy Shallow Bay Fill	If(Sand_fine>=0.36 And Sand_fine<=0.38 Or Silt>=0.18 And Silt<=0.2 Or Clay>0.18 And Clay<=0.19 Or Depth_of_deposition>=-30 And Depth_of_deposition<=-20)
2	Sandy Shallow Bay Fill	If(Sand_coarse>=0.65 And Sand_coarse<=0.73 Or Sand_fine>=0.18 And Sand_fine<=0.22 Or Silt>=0.18 And Silt<=0.2 Or Clay>=0.17 And Clay<=0.18 Or Depth_of_deposition>=-3 And Depth_of_deposition<=0)
3	Channel Fill Sandstone	If(Sand_coarse>=0.5 And Sand_coarse<=0.68 Or Sand_fine>=0.23 And Sand_fine<=0.25 Or Silt>=0.17 And Silt<=0.18 Or Depth_of_deposition>=0 And Depth_of_deposition<=2)
4	Lower Shoreface Units	If(Sand_coarse>=0.19 And Sand_coarse<=0.31 Or Sand_fine>=0.19 And Sand_fine<=0.24 Or Silt>=0.4 And Silt<=0.48 Or Clay>=0.19 And Clay<=0.31 Or Depth_of_deposition>=-83 And Depth_of_deposition<=50)
5	Middle Shoreface Units	If(Sand_coarse>=0.32 And Sand_coarse<=0.53 Or Sand_fine>=0.25 And Sand_fine<=0.32 Or Silt>=0.26 And Silt<=0.32 Or Clay>=0.19 And Clay<=0.21 Or Depth_of_deposition>=-38 And Depth_of_deposition<=-12)
6	Upper Shoreface Units	If(Sand_coarse>=0.53 And Sand_coarse<=0.72 Or Sand_fine>=0.28 And Sand_fine<=0.33 Or Silt>=0.16 And Silt<=0.21 Or Depth_of_deposition>=-10 And Depth_of_deposition<=6)
7	Distal Mouth Bar Units	If(Sand_fine>=0.23 And Sand_fine<=0.27 Or Silt>=0.38 And Silt<=0.43 Or Clay>=0.19 And Clay<=0.21 Or Depth_of_deposition>=-95 And Depth_of_deposition<=-80)
8	Proximal Mouth Bar Units	If(Sand_coarse>=0.53 And Sand_coarse<=0.71 Or Sand_fine>=0.27 And Sand_fine<=0.32 Or Silt>=0.16 And Silt<=0.21 Or Clay>=0.06 And Clay<=0.07 Or Depth_of_deposition>=-30 And Depth_of_deposition<=-27)
9	Tide Influenced Sandstones	If(Sand_coarse>=0.53 And Sand_coarse<=0.71 Or Sand_fine>=0.26 And Sand_fine<=0.31 Or Silt>=0.35 And Silt<=0.41 Or Depth_of_deposition>=-5 And Depth_of_deposition<=1)
10	Fluvial Channel Sandstones	If(Sand_coarse>=0.54 And Sand_coarse<=0.56 Or Sand_fine>=0.27 And Sand_fine<=0.29 Or Silt>=0.19 And Silt<=0.21 Or Depth_of_deposition>=-2 And Depth_of_deposition<=2)
11	Coal	Estimated as background attribute
12	Coastal plain fines	If(Silt>=0.31 And Silt<=0.43 Or Clay>=0.31 And Clay<=0.35 Or Depositional_depth>=-100 And Depositional_depth<=-40)
13	Marine Mudstone	If(Sand_fine>=0.36 And Sand_fine<=0.38 Or Silt>=0.4 And Silt<=0.52 Or Clay>=0.45 And Clay<=0.78 Or Depth_of_deposition>=-105 And Depth_of_deposition<=-90)

Lithofacies Classification

Facies Code	Lithofacies	Command Used in Petrel's Property Calculator
0	Marine Shale	If(Sand_fine>=0.19 And Sand_fine<=0.21 Or Silt>=0.19 And Silt<=0.2 Or Clay>=0.2 And Clay<=0.21 Or Depth_of_deposition>=-82 And Depth_of_deposition<=-78)
1	Muddy Shallow Bay Fill	If(Sand_fine>=0.36 And Sand_fine<=0.38 Or Silt>=0.18 And Silt<=0.2 Or Clay>0.18 And Clay<=0.19 Or Depth_of_deposition>=-30 And Depth_of_deposition<=-20)
2	Sandy Shallow Bay Fill	If(Sand_coarse>=0.65 And Sand_coarse<=0.73 Or Sand_fine>=0.18 And Sand_fine<=0.22 Or Silt>=0.18 And Silt<=0.2 Or Clay>=0.17 And Clay<=0.18 Or Depth_of_deposition>=-3 And Depth_of_deposition<=0)
3	Channel Fill Sandstone	If(Sand_coarse>=0.5 And Sand_coarse<=0.68 Or Sand_fine>=0.23 And Sand_fine<=0.25 Or Silt>=0.17 And Silt<=0.18 Or Depth_of_deposition>=0 And Depth_of_deposition<=2)
4	Lower Shoreface Units	If(Sand_coarse>=0.19 And Sand_coarse<=0.31 Or Sand_fine>=0.19 And Sand_fine<=0.24 Or Silt>=0.4 And Silt<=0.48 Or Clay>=0.19 And Clay<=0.31 Or Depth_of_deposition>=-83 And Depth_of_deposition<=50)
5	Middle Shoreface Units	If(Sand_coarse>=0.32 And Sand_coarse<=0.53 Or Sand_fine>=0.25 And Sand_fine<=0.32 Or Silt>=0.26 And Silt<=0.32 Or Clay>=0.19 And Clay<=0.21 Or Depth_of_deposition>=-38 And Depth_of_deposition<=-12)
6	Upper Shoreface Units	If(Sand_coarse>=0.53 And Sand_coarse<=0.72 Or Sand_fine>=0.28 And Sand_fine<=0.33 Or Silt>=0.16 And Silt<=0.21 Or Depth_of_deposition>=-10 And Depth_of_deposition<=6)
7	Distal Mouth Bar Units	If(Sand_fine>=0.23 And Sand_fine<=0.27 Or Silt>=0.38 And Silt<=0.43 Or Clay>=0.19 And Clay<=0.21 Or Depth_of_deposition>=-95 And Depth_of_deposition<=-80)
8	Proximal Mouth Bar Units	If(Sand_coarse>=0.53 And Sand_coarse<=0.71 Or Sand_fine>=0.27 And Sand_fine<=0.32 Or Silt>=0.16 And Silt<=0.21 Or Clay>=0.06 And Clay<=0.07 Or Depth_of_deposition>=-30 And Depth_of_deposition<=-27)
9	Tide Influenced Sandstones	If(Sand_coarse>=0.53 And Sand_coarse<=0.71 Or Sand_fine>=0.26 And Sand_fine<=0.31 Or Silt>=0.35 And Silt<=0.41 Or Depth_of_deposition>=-5 And Depth_of_deposition<=1)
10	Fluvial Channel Sandstones	If(Sand_coarse>=0.54 And Sand_coarse<=0.56 Or Sand_fine>=0.27 And Sand_fine<=0.29 Or Silt>=0.19 And Silt<=0.21 Or Depth_of_deposition>=-2 And Depth_of_deposition<=2)
11	Coal	Estimated as background attribute
12	Coastal plain fines	If(Silt>=0.31 And Silt<=0.43 Or Clay>=0.31 And Clay<=0.35 Or Depositional_depth>=-100 And Depositional_depth<=-40)
13	Marine Mudstone	If(Sand_fine>=0.36 And Sand_fine<=0.38 Or Silt>=0.4 And Silt<=0.52 Or Clay>=0.45 And Clay<=0.78 Or Depth_of_deposition>=-105 And Depth_of_deposition<=-90)

Table 4. Porosity and Permeability ~~estimate in identified~~ estimates of lithofacies packages in the model area.

Code	Lithofacies	Average NPHI	Density Porosity	Estimated Porosity	KLOGH (mD)
0	Marine Shale	0.17 - 0.45	0.1	0.08 - 0.11	10.02 - 16.1
1	Muddy Shallow Bay Fill	0.17 - 0.42	0.1	0.08 - 0.13	23.85 - 102.3
2	Sandy Shallow Bay Fill	0.07 - 0.52	0.25	0.16 - 0.25	100.0 - 398.7
3	Channel Fill Sandstone	0.04 - 0.15	0.30	0.18 - 0.22	400.01 - 889.7
4	Distal Lower Shoreface	0.04 - 0.19	0.29	0.1 - 0.23	120.5 - 170.3
5	Proximal Shoreface	0.05 - 0.17	0.31	0.17 - 0.24	80.2 - 412.5
6	Upper Shoreface Units	0.09 - 0.11	0.28	0.21 - 0.26	650.2 - 1023.7
7	Distal Mouth Bar Units	0.08 - 0.17	0.27	0.09 - 0.17	170.5 - 223.1
8	Proximal Mouth Bar	0.05 - 0.59	0.12	0.19 - 0.21	130.5 - 314.3
9	Tide Influenced SS	0.14 - 0.46	0.26	0.15 - 0.20	220.0 - 512.6
10	Fluvial Sandstones	0.14 - 0.29	0.21	0.19 - 0.21	180.5 - 691.8
11	Coal	0.24 - 0.53	0.05	0.001	0.001
12	Coastal Plain Fines	0.43 - 0.49	0.06	0.04 - 0.12	5.2 - 34.6
13	Marine Mudstone	0.16 - 0.42	0.1	0.08 - 0.10	6.0 - 15.2

Code	Lithofacies	Avg. NPHI	Density Porosity	Estimated Porosity	KLOGH (mD)
0	Marine Shale	0.17 - 0.45	0.1	0.08 - 0.11	10.02 - 16.1
1	Muddy Shallow Bay Fill	0.17 - 0.42	0.1	0.08 - 0.13	23.85 - 102.3
2	Sandy Shallow Bay Fill	0.07 - 0.52	0.25	0.16 - 0.25	100.0 - 398.7
3	Channel Fill Sandstone	0.04 - 0.15	0.3	0.18 - 0.22	400.01 - 889.7
4	Distal Lower Shoreface	0.04 - 0.19	0.29	0.1 - 0.23	120.5 - 170.3
5	Proximal Shoreface	0.05 - 0.17	0.31	0.17 - 0.24	80.2 - 412.5
6	Upper Shoreface	0.09 - 0.11	0.28	0.21 - 0.26	650.2 - 1023.7
7	Distal Mouth Bar	0.08 - 0.17	0.27	0.09 - 0.17	170.5 - 223.1
8	Proximal Mouth Bar	0.05 - 0.59	0.12	0.19 - 0.21	130.5 - 314.3
9	Tidal Influenced Sandstone	0.14 - 0.46	0.26	0.15 - 0.20	220.0 - 512.6
10	Fluvial Sandstones	0.14 - 0.29	0.21	0.19 - 0.21	180.5 - 691.8
11	Coal	0.24 - 0.53	0.05	0.001	0.001
12	Coastal Plain Fines	0.43 - 0.49	0.06	0.04 - 0.12	5.2 - 34.6
13	Marine Mudstone	0.16 - 0.42	0.1	0.08 - 0.10	6.0 - 15.2

Table 5. ~~Comparison~~**A** comparison of a) porosity, and b) permeability estimates ~~in~~ from selected intervals in the original ~~petrophysical model~~porosity/permeability models and forward modeling-based porosity and permeability models.

a. Validation Well Position 1							
	Porosity: GPM-Based Model					Porosity: Original Model	
	Depth (m)						
Models	5 m	10 m	15 m	25 m	35 m	Depth (m)	Average Porosity
R14	0.22	0.24	0.16	0.22	0.16	5	0.2
R20	0.16	0.19	0.26	0.18	0.15	10	0.25
R26	0.18	0.17	0.23	0.16	0.19	15	0.27
R36	0.22	0.21	0.19	0.22	0.21	25	0.16
R45	0.25	0.2	0.23	0.22	0.15	35	0.13
R49	0.21	0.17	0.22	0.17	0.18		
Validation Well Position 2							
	Porosity: GPM-Based Model					Porosity: Original Model	
	Depth (m)						
Models	5 m	10 m	15 m	25 m	35 m	Depth (m)	Average Porosity
R14	0.17	0.16	0.24	0.15	0.25	5	0.17
R20	0.21	0.22	0.2	0.21	0.23	10	0.21
R26	0.21	0.2	0.21	0.25	0.24	15	0.21
R36	0.2	0.22	0.21	0.21	0.19	25	0.17
R45	0.22	0.19	0.2	0.19	0.21	35	0.19
R49	0.26	0.24	0.23	0.16	0.21		

b. Validation Well Position 1							
	Permeability_Z (mD): GPM-Based Model					Permeability_Z: Original Model	
	Depth (m)						
Models	5 m	10 m	15 m	25 m	35 m	Depth (m)	Average Perm_Z
R14	163.95	312.38	69.84	310.16	508.2	5	352.74
R20	290.84	315.09	105.66	273.04	200.63	10	312.38
R26	375.92	203.81	166.23	189.92	348.12	15	201.08
R36	418.03	203.27	190.9	168.9	370.56	25	199.76
R45	337.6	412.67	199.66	156.71	305.92	35	508.2
R49	370.89	129.33	291.77	175.53	551.18		
Validation Well Position 2							
	Permeability_Z (mD): GPM-Based Model					Permeability_Z: Original Model	
	Depth (m)						
Models	5 m	10 m	15 m	25 m	35 m	Depth (m)	Average Perm_Z
R14	320.34	336.22	151.08	464.22	132.98	5	6.6
R20	122.66	209.15	161.3	230.58	208.48	10	883.6
R26	151.48	710.07	175.09	384.49	169.48	15	30.3
R36	184.74	344.99	157.08	420.15	136.14	25	496.99
R45	91.44	361.04	77.17	382.85	134.56	35	156.6
R49	134.01	721.73	137.42	636.48	290.06		

a. Validation Well Position 1					
	Depth (m)				
	5 m	10 m	15 m	25 m	35 m
Models	**Measured Porosity**				
Original Model	0.2	0.25	0.27	0.16	0.13
R14	0.22	0.24	0.16	0.22	0.16
R20	0.16	0.19	0.26	0.18	0.15
R26	0.18	0.17	0.23	0.16	0.19
R36	0.22	0.21	0.19	0.22	0.21